63

N70 33074

Contract NAS9-9579 NASA CR-108457

FINAL REPORT

EXPERIMENTAL STUDY OF POP-IN BEHAVIOR OF SURFACE FLAW-TYPE CRACKS

By

Fred R. Schwartzberg, Richard H. Gibb, Emory J. Beck

JULY 1970

Prepared for

NATIONAL AERONAUTICS AND SPACE ADMINISTRATION
MANNED SPACECRAFT CENTER
HOUSTON, TEXAS

Technical Management

R. G. FORMAN

MARTIN MARIETTA DENVER DIVISION

CASE FILE COPY

NOTICE

This report was prepared as an account of Government sponsored work. Neither the United States, nor the National Aeronautics and Space Administration (NASA), nor any person acting on behalf of NASA:

(A) Makes any warranty or representation, expressed or implied, with respect to the accuracy, completeness, or usefulness of the information contained in this report, or that the use of any information, apparatus, method, or process disclosed in this report may not infringe privately owned rights; or

(B) Assumes any liabilities with respect to the use of, or for damages resulting from the use of any information, apparatus, method or process disclosed in this report.

As used above, "person acting on behalf of NASA" includes any employee or contractor of NASA, or employee of such contractor, to the extent that such employee or contractor of NASA, or employee of such contractor prepares, disseminates, or provides access to, any information pursuant to his employment or contract with NASA, or his employment with such contractor.

Requests for copies of this report should be referred to:

National Aeronautics and Space Administration
Office of Scientific and Technical Information

Attention: AFSS-A
Washington, D.C. 20546

NASA CR-108457

Contract NAS9-9579

FINAL REPORT

EXPERIMENTAL STUDY OF POP-IN BEHAVIOR OF SURFACE FLAW-TYPE CRACKS

July 1970

by

Fred R. Schwartzberg, Richard H. Gibb, Emory J. Beck

Prepared for

NATIONAL AERONAUTICS AND SPACE ADMINISTRATION
MANNED SPACECRAFT CENTER
HOUSTON, TEXAS

R. G. Forman
Technical Management

MARTIN MARIETTA CORPORATION
P. O. Box 179
Denver, Colorado 80201

FOREWORD

This final report was prepared by Martin Marietta Corporation under Contract NAS9-9579, *Experimental Study of Pop-in Behavior of Surface Flaw-Type Cracks*, for the Manned Spacecraft Center of the National Aeronautics and Space Administration. This work was administered under the direction of Mr. R. G. Forman at NASA/MSC.

Mr. Fred R. Schwartzberg served as Martin Marietta Program Manager and Mr. Richard H. Gibb as Technical Director. Mr. Emory J. Beck served as fracture mechanics consultant.

ABSTRACT

Titanium alloy 6Aℓ-4V STA was evaluated in order to determine whether flaw growth occurring during proof testing of hardware results from pop-in or slow growth. The factors that affect such growth and the effect of subsequent service life were also determined.

The results showed that crack extension was of the slow growth type, initiating at stress intensities above $85\%K_{Ic}$. Growth was found to be minor at cryogenic temperatures and modest at room temperature. It was concluded that the susceptibility to slow growth is strongly influenced by crack size.

The great value of the cryogenic proof test was confirmed.

CONTENTS

Figure

SUMMARY

The objective of this program was to characterize the behavior of 6Al-4V STA titanium alloy in order to satisfy the following requirements:

1) To determine whether flaw growth occurrence during proof testing results from environmental effects (e.g., slow growth caused by stress corrosion) or from pop-in where the crack extends initially in a state of plane strain and is arrested when the state changes to plane stress;

2) To determine the effect of stress-intensity-factor level, plate thickness, flaw shape, flaw location, and environment on the occurrence of flaw growth during proof testing;

3) To determine the effect of flaw growth during proof testing on the remaining cyclic life at normal operating stress levels.

Flaw growth during proof testing was of the slow growth type. Although the occurrence of slow flaw growth implies a stress corrosion mechanism, our data does not indicate a sufficient difference in the susceptibility to slow growth to firmly show an environmental effect in comparing the various media.

Tunneling behavior, as described in prior work by others, was neither prevalent nor significant. The magnitude of tunneling was not great; in most cases it was manifest by little more than a tendency to square off the semielliptical-shaped precrack. Tunneling behavior, under slow growth conditions, appears to be more prevalent with a high a/2c ratio in the gages tested.

It was determined that the level at which flaw growth initiated was 85 to 90% of the critical stress intensity $\left(K_{Ic}\right)$.

At 70°F, slow growth was significant at high percentages of K_{Ic} and under longtime holding. Cryogenic tests showed that growth was quite minor at similar levels of stress intensity. This observation has caused us to conclude that the susceptibility to slow growth is strongly influenced by crack size, since the LN_2 specimens contained small flaws and did not exhibit great growth.

Based on the slow growth observations, it is important that static fracture toughness data be obtained so that failures occur in the stress range corresponding to the anticipated proof stress. For the Apollo hardware, this implies 70°F static toughness tests in the 140 ksi range and -320°F tests in the 187 ksi range. For the flaw sizes that will cause failures at these stresses, slow flaw growth is not significant.

The data generated in this program confirms the great value of the cryogenic proof tests for establishing the highest possible reliability in hardware. It is also apparent that a room temperature proof test prior to cryogenic proof testing is still a satisfactory technique to screen out the larger flaws. There is the possibility, although not great, that the room temperature proof test may result in leakage rather than catastrophic failure; there is no probability of the large flaws passing the cryogenic proof test.

I. INTRODUCTION

The application of fracture mechanics technology to the qualification of pressure vessel hardware is commonly achieved by utilization of the proof test method. Basically, this approach uses the logic that a proof test can provide information on the maximum flaw size that could be present in the structure. A comparison of this flaw size with that required to cause failure at the service stress, and evaluation of the tendency toward slow crack growth under sustained or cyclic loading, presumably gives a valid measure of the reliability of the hardware.

In certain situations, particularly with deep flaws in thin-gage high-toughness materials, there is the probability that the proof test method does not fully characterize behavior because of "pop-in"* or slow crack growth. The possibility exists that cracks of larger magnitude than those predicted can be present after proof testing. It is therefore essential that the growth characteristics of such defects be fully evaluated in order to predict structural reliability.

The objective of this program is to study the flaw growth behavior in 6Aℓ-4V titanium alloy resulting from stress profiles similar to those which occur during proof testing of the Apollo spacecraft pressure vessel.

*arrested crack growth

II. BACKGROUND

Unexpected failures of Apollo pressure vessel hardware that occurred in late 1966 focused attention on the reliability of such hardware. As a result, research was initiated to determine the suitability of fracture mechanics techniques to predict performance.

Three programs, conducted by Boeing to investigate flaw growth behavior (Ref 1, 2, and 3), dealt with the effect of various environments on the sustained load flaw growth and with cyclic load growth behavior.

A fourth program, performed by Battelle Memorial Institute (Ref 4), dealt with an experimental program to: (1) determine the feasibility of using the cryogenic proof test to screen out small defects; (2) establish maximum anticipated defect size after proof testing; (3) study flaw growth behavior; (4) study environmental effects; and (5) study the relationship between thickness and flaw tolerance. The Battelle findings led to the conclusion that the cryogenic proof test would indeed point to the detection of smaller flaws than could be found by a room-temperature proof test. It was also found that subcritical cracks that did not cause failure in proof would grow during lower stress cyclic loading (105 ksi), but that the critical crack size was greater than the wall thickness so that leakage would precede catastrophic failure. The principal observation made in this program was the pop-in behavior or tunneling growth that occurred in the width direction during proof testing. As a result of the findings of this program, it was recommended that a further study of the effect of flaw growth during proof testing be performed. This recommendation was the basis for the current investigation.

III. EXPERIMENTAL PLAN

The objective of this investigation was to characterize the effect of flaw geometry, location, material thickness, environment, and proof stress hold time on flaw growth behavior of 6Aℓ-4V STA titanium alloy. Specifically, the program goals were to determine:

1) Whether flaw growth occurrence during proof testing results from environmental effects (e.g., slow growth caused by stress corrosion) or from pop-in where the crack initially extends in a state of plane strain and is arrested when the state changes to plane stress;
2) The effect of stress-intensity factor level, thickness, flaw shape, flaw location on the occurrence of flaw growth during proof testing;
3) The effect of flaw growth during proof testing on the remaining cyclic life at normal operating stress levels.

The procedure used in this program was to apply the proof stress profile depicted in Figure III-1 to various titanium specimens, and then fatigue-cycle the specimens to determine the effect of growth during proof testing.

Specimens were to be prepared and evaluated according to the following conditions in order to characterize the desired behavior:

1) Test material and condition

   Alloy - 6Aℓ-4V titanium alloy,

   Condition - STA (solution treated and aged) plus stress relief (1000°F/4 hr, AC) after specimen machining,

   Thickness - nominal thicknesses of 0.032, 0.063, and 0.090 inch;

2) Flaw geometry

   Normal flaw - $a/2c \simeq 0.4$,

   Elongated flaw - $a/2c = 0.1$ to 0.2;

3) Flaw location

   Parent metal,

   Weld centerline,

   Heat affected zone;

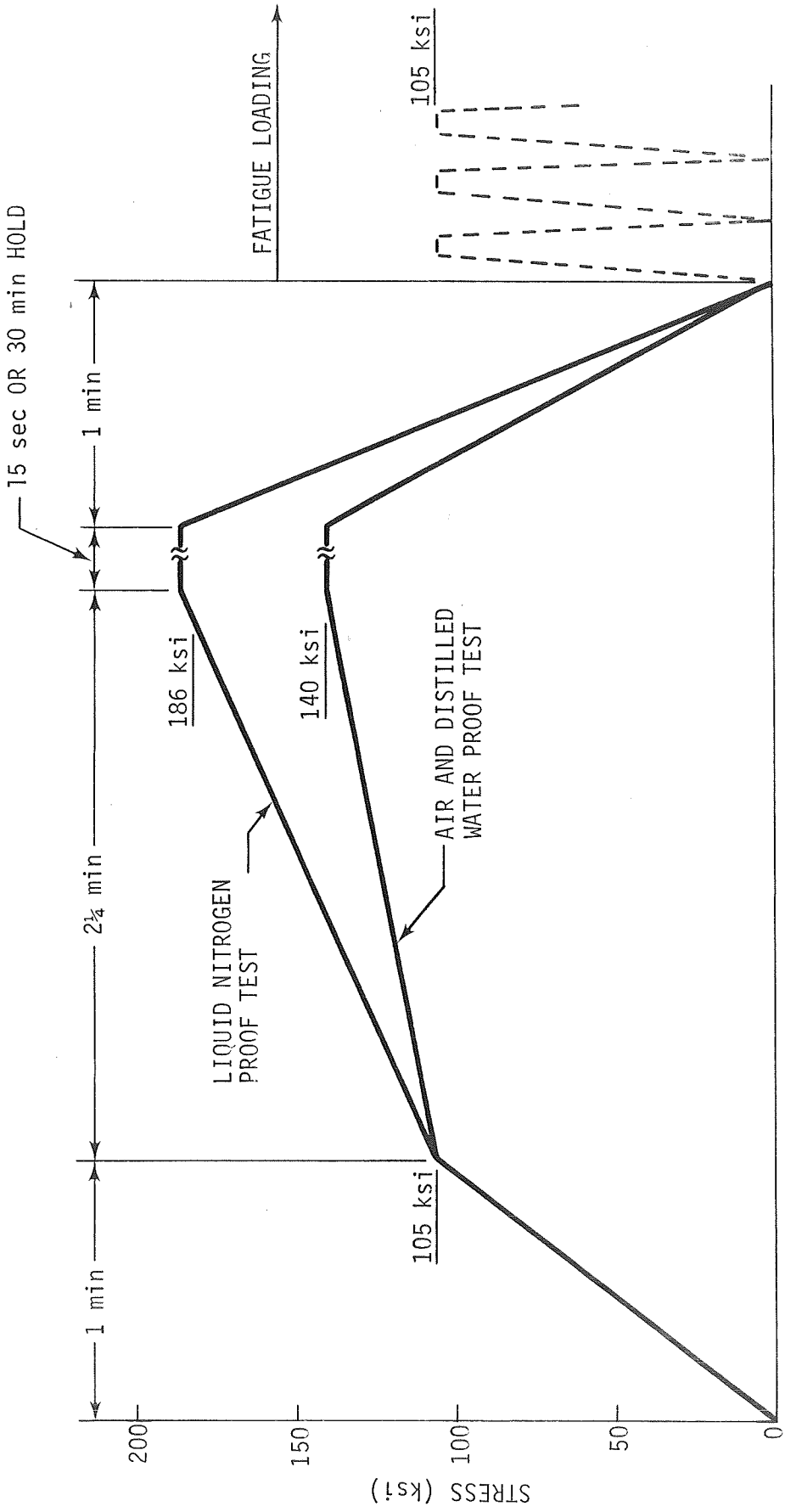

Figure III-1 Proof and Fatigue Loading Profile

4) Environments

50% relative humidity air,

Distilled water,

Liquid nitrogen;

5) Flaw growth measuring techniques

Strain gages,

Compliance gage,

Optical microscope,

Accelerometer;

6) Proof stress and stress intensity

Nominal proof stress

70°F = 140 ksi
-320°F = 186 ksi,

Initial stress intensity

K_{Ii} = 0.85 to 1.00 K_{Ic}.

IV. MATERIALS PROCESSING

A. MATERIAL

The titanium alloy sheet (6Aℓ-4V) material was supplied as government furnished property by NASA-MSC. All material was produced by Titanium Metals Corporation of America (TMCA) and was furnished in the solution-treated and aged condition. Although it was originally intended for all material of a single gage to be furnished from a single heat, this was not possible. As a result, two heats were used for the 0.063-inch gage testing; heat G-8202 was used for welded specimens, heat K-2312 was used for parent metal testing.

TMCA's certification report listed the composition and properties given in Table IV-1.

Table IV-1 Vendor's Certification Data

HEAT NO.	GAGE (in.)	COMPOSITION (wt %)							MECHANICAL PROPERTIES		
		C	Fe	N_2	Aℓ	V	H_2	O_2	ULTIMATE STRENGTH (ksi)	YIELD STRENGTH (ksi)	ELONGATION (%)
G-6570	0.090	0.022	0.09	0.010	6.0	4.0	0.008	0.11	170.7	160.9	9.0
G-8202	0.063	0.023	0.09	0.013	5.9	3.9	0.008	0.12	176.8	166.0	7.0
K-2312	0.063	0.026	0.07	0.015	6.0	4.0	0.007	0.11	164.7	153.9	8.5
K-2312	0.032	0.026	0.07	0.015	6.0	4.0	0.008	0.11	164.2	155.6	8.0

B. WELDING

Panels were prepared for welding in the following manner. First, the alloys were degreased in trichloroethylene vapor, soaked in an alkaline solution for 15 minutes, deoxidized in HNO_3-HF pickling solution for 5 minutes, and rinsed in demineralized water. Then the edges were filed, the corners were broken slightly, and

finally the surface next to the edge was sanded lightly with 180-grit paper. The specimens were welded transverse to the grain direction using a direct-current, straight-polarity, 600-amp Sciaky Zero Error supply and an Airline welding fixture. Welding was achieved with a single pass using 0.045-inch diameter commercial-purity titanium filler wire. Welding parameters are tabulated.

Welding Parameters	Gage (in.)		
	0.090	0.063	0.032
Current, amp	110	98	35
Voltage, v	12	7.8	7.8
Torch speed, ipm	6	7	9.5
Wire feed, ipm	15	8	10
Torch gas, argon, cfh	50	30	30
Trailer gas, argon, cfh	45	45	45
Backup gas, argon, cfh	13	13	13
Hold-down plates, distance from ℄, in.	3/8	5/16	3/16
Electrode diameter 2% thoria, in.	0.125	0.125	0.062

Subsequent radiographic inspection showed no evidence of defects or porosity and the welds were declared acceptable.

C. FINAL PROCESSING

Specimens were stress relieved after final machining, but prior to electro-discharge machining (EDM). The entire sequence is as follows. First, the as-received specimens were deburred with 600-grit metallographic polishing paper. Then they were cleaned according to the same procedure used prior to welding. Specimens were coated with Turco pretreat to prevent oxidation during the stress relieving operation. Stress relieving was accomplished at 1000°F for 4 hours in a circulating air furnace; and specimens were air-cooled. The surface was then cleaned by vapor honing and HNO_3-HF pickling treatment.

The flaw starter was then placed in the specimens using the EDM technique. After the EDM process, specimens were given a final cleaning in acetone prior to fatigue extension of the precracks.

V. EXPERIMENTAL PROCEDURE AND TECHNIQUES

A. MECHANICAL PROPERTY TESTING

1. Specimen Design

Two types of specimen designs were used in this investigation. Room temperature specimens were of the standard friction-gripped design specified in ASTM-E-8; the cryogenic specimens used the same test gage but contained pin-loading grip ends (Fig. V-1).

Weld beads were machined flush.

2. Instrumentation

Bonded resistance strain gages were used to obtain load vs strain data. Series-connected gages, mounted on opposite surfaces, were used to compensate for small misalignments and bending on parent metal specimens. Weld specimens were tested with single miniature (1/32-in.) gages; the gage was located at the desired position on the weld zone (weld bead centerline or heat affected zone).

Strain gages were used to establish a full bridge circuit of strain gages and to compensate for temperature effects in the bridge by bonding the strain gages to dummy boards made of the same type of material being evaluated. For cryogenic testing, the entire bridge is submerged in the liquid. Using this technique, no external resistors or balancing systems are required. Constantan gages were used for 70°F testing; for cryogenic testing, nichrome gages were used.

3. Testing Procedure

Tensile specimens were tested in laboratory air at 70°F and at -320°F using a liquid nitrogen bath in an open-mouthed, foam insulated cryostat. Because of the tendency for cryogenic test specimens to fail prematurely through punched gage marks and the primary need for yield strength data to be used in fracture toughness calculations, no elongation data were obtained in the -320°F tests.

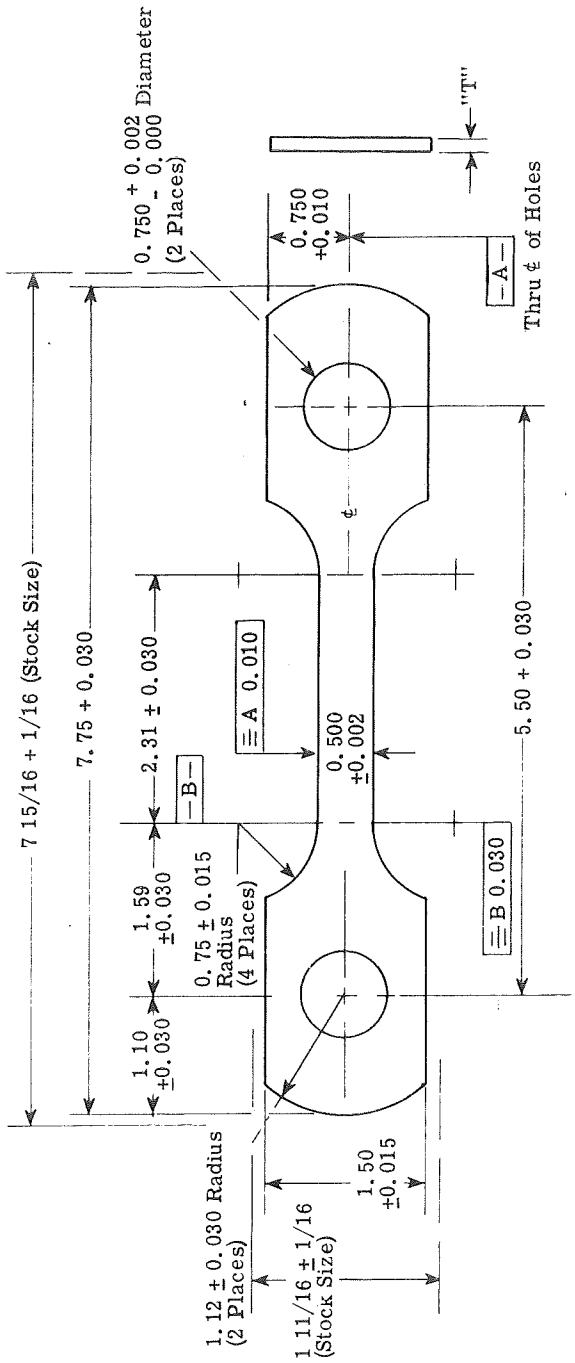

Figure V-1 Specifications for Cryogenic Tensile Specimen

B. FRACTURE TESTING

1. Specimen Design

The original plans called for evaluation of a 3-inch wide test specimen. However, failure to obtain sufficient titanium alloy necessitated a change to a slightly smaller specimen. The design selected, shown in Figure V-2, utilized a 2.3-inch gage width. Triple pin loading was used.

2. Specimen Preparation

In all welded specimens, the weld bead was machined flush with the surface.

Surface flaws were introduced into the specimens by electro-discharge machining the starter flaw and extending by fatigue loading. Two types of starter flaws were introduced by the EDM process for the normal flaw ($a/2c \simeq 0.4$), the starter was introduced by using a 0.003-inch diameter tungsten wire and machining to the required depth. The elongated flaws ($a/2c = 0.1$ to 0.2 were introduced with a shaped tool fabricated from 0.010-inch thick tungsten-copper; the cutting edge of this tool was shaped (to the required a/2c ratio) and sharpened by hand.

The EDM starter cracks were then fatigue-extended. All specimens were initially fatigued in 3-point bending using a Wiedeman-Sonntag SF-IU machine, and a 2-inch beam span was utilized at an outer fiber stress not exceeding 90 ksi. Final fatigue extension of all room temperature specimens requiring the 0.4 a/2c ratio was conducted in axial tension in a Marquardt TM-1 machine at a nominal stress of 50 ksi. The flaws required for the liquid nitrogen specimens did not require axial loading to achieve the desired shape.

3. Control of Crack Geometry

An extensive program was performed to ensure accurate control of crack geometry. This was required because the proof test exposure required both stress and stress intensity to be fixed parameters. This can only be achieved by accurately controlling crack depth and shape.

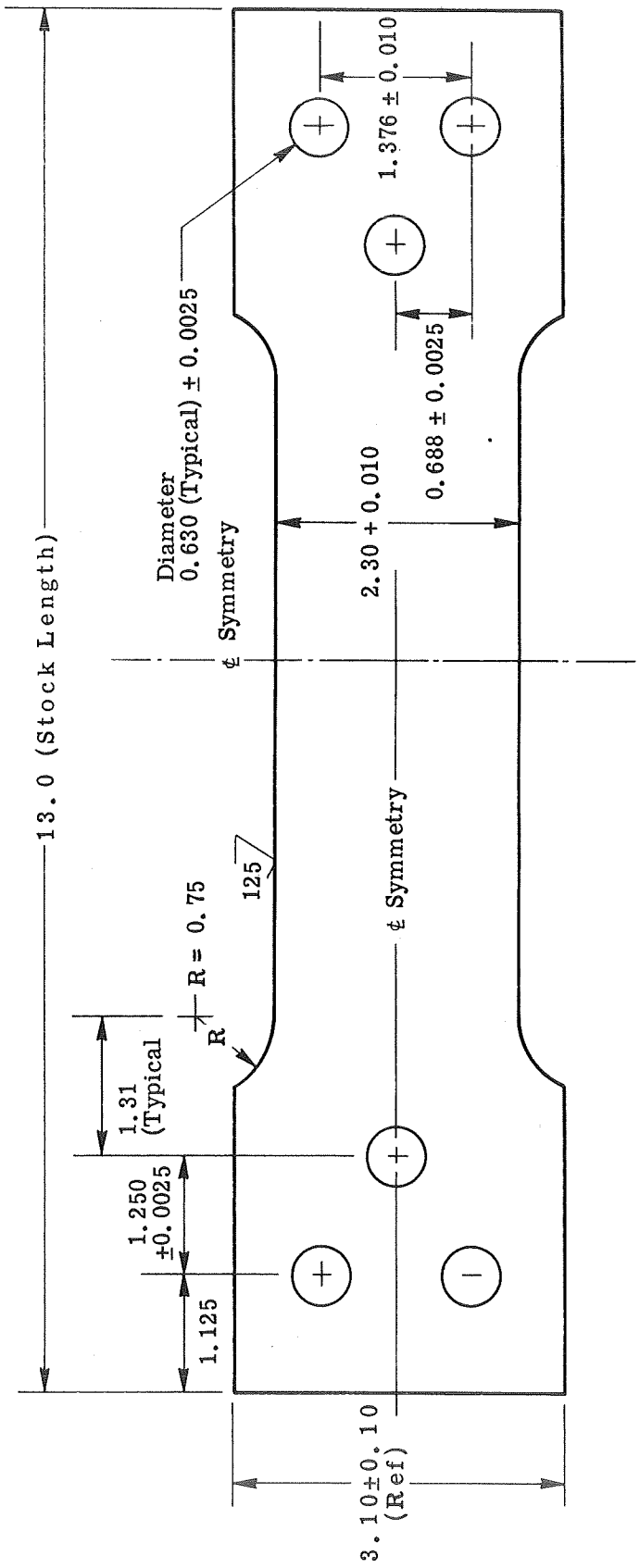

Figure V-2 Specifications for Surface-Flawed Fracture Toughness Specimens

In order to achieve this level of control, several hundred test strips of the 2.3-inch specimen gage width were prepared. EDM starters were introduced and specimens were fatigued and then opened to determine crack depth and shape. The following critical variables were controlled: starter flaw dimensions, cyclic stress, and gage thickness. As a result of this effort, we could then select the starter flaw dimensions necessary to achieve the desired flaw crack depth and shape.

4. Instrumentation

Normally, no instrumentation is used when testing surface-flawed specimens. However, because of our desire to detect pop-in behavior it was necessary to provide extensive instrumentation in order to ensure detection of any precritical flaw growth.

In prior work (Ref 5), we developed the technique for using small resistance strain gages placed near the edge of the crack to detect pop-in behavior. For this work, 1/32-inch grid length gages were utilized; Micro-Measurements EA-06-031DE-120 gages were used at 70°F and EK-06-031DE-350 gages at -320°F. Gages were located approximately 0.5-crack lengths (2c) from the edge of the fatigued crack. Strain versus load readout was accomplished using a Mosley 2D-2A X-Y plotter.

A second method used to detect pop-in or crack growth was a compliance gage. We used a modified Instron strain gage beam extensometer for the room temperature tests and a specially designed and constructed sensing unit with nichrome gages for -320°F testing. The room temperature unit was attached to the specimen by seating the gage points into small conical indentations punched into the specimen; a 0.1-inch gage length was used (Fig. V-3). The cryogenic gage was clipped to the specimen by using small tabs that were adhesively bonded to the specimen across the flaw; Figure V-4 shows this arrangement. The output of the compliance gage was amplified by a low-noise limited bandwidth preamplifier and fed into an X-Y plotter. It was difficult to attain the desired performance of the compliance gage system because of noise generated in the amplifier system and some degree of mechanical instability.

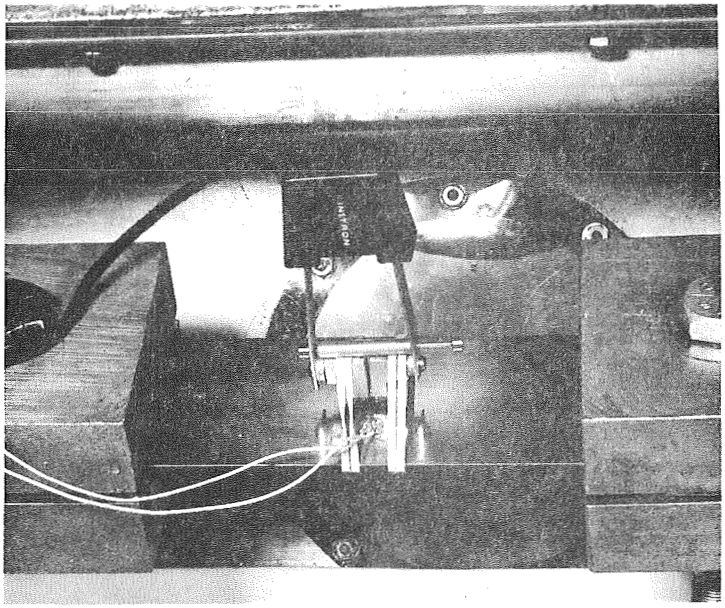

Figure V-3 Closeup View of Room Temperature Compliance Gage

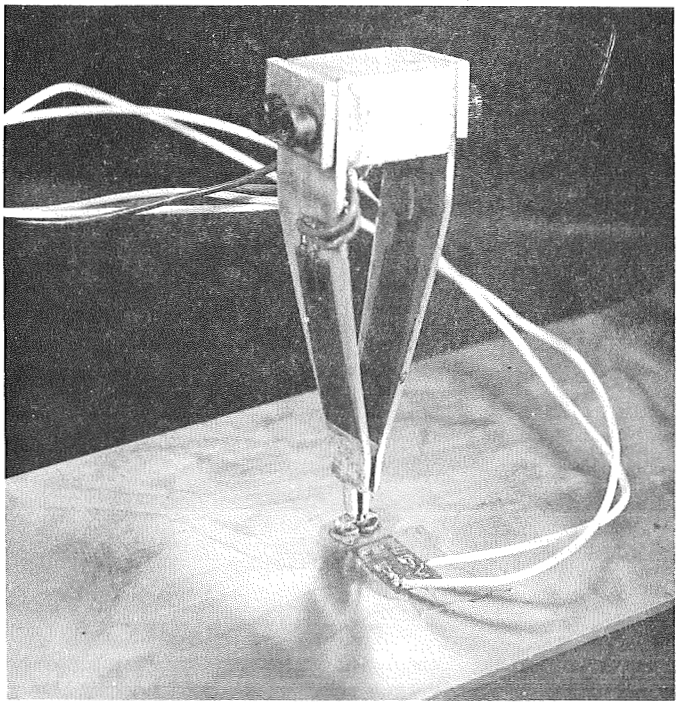

Figure V-4 Closeup View of Cryogenic Compliance Gage

The third instrumentation method was the accelerometer system used to acoustically monitor flaw growth. An Endevco model 2213C accelerometer with a sensitivity of 43 peak mv/peak g was used. The readout of the accelerometer was accomplished on a Tektronix type 564B storage oscilloscope. Initially, a charge amplifier was used in conjunction with an Ampex tape recorder; however, it was found that the charge amplifier exhibited an electronic failure due to overloading each time the specimen failed. As a result it was necessary to develop an alternative instrumentation system. It was found that adequate sensitivity could be achieved with the Tektronix preamplifier and storage scope. Visual observations made on the oscilloscope were recorded by event marking a time versus load plot on a third X-Y plotter.

The fourth system for detecting flaw growth was visual observation. This was achieved by viewing the backface of the specimen using a stereo microscope at a magnification of 20X.

5. Testing Apparatus

A Marquardt model TM-1 50,000-pound servo-controlled, electro-hydraulic universal testing machine was used for static K_{Ic}, proof and cyclic growth testing at both 70 and -320°F. Figure V-5 shows an overall view of this machine. The automatic programer contained in this machine was used to control the proof loading cycle. Figure V-6 gives a closeup view of the programer and shows the load versus time profile used for this work.

Cyclic growth testing was achieved using the same machine except that a Research, Inc. Data-Trak programer was used to provide the trapezoid pattern load impulse to the TM-1. A cycling rate of 14 cycles/minute with a peak hold time of 1.3 seconds was used for this testing. Figure V-7 shows the Data-Trak unit.

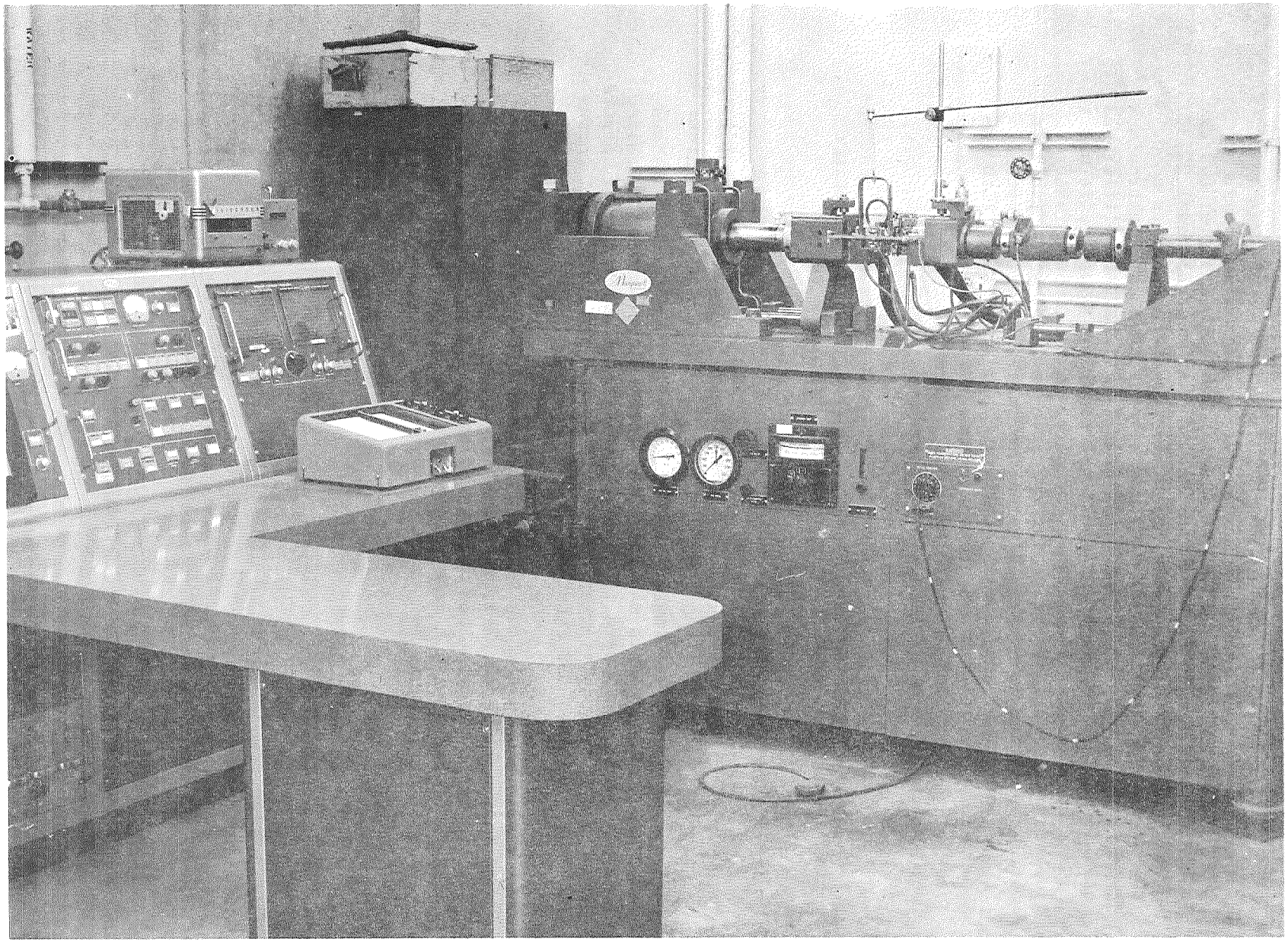

Figure V-5 Marquardt TM-1 Testing Machine

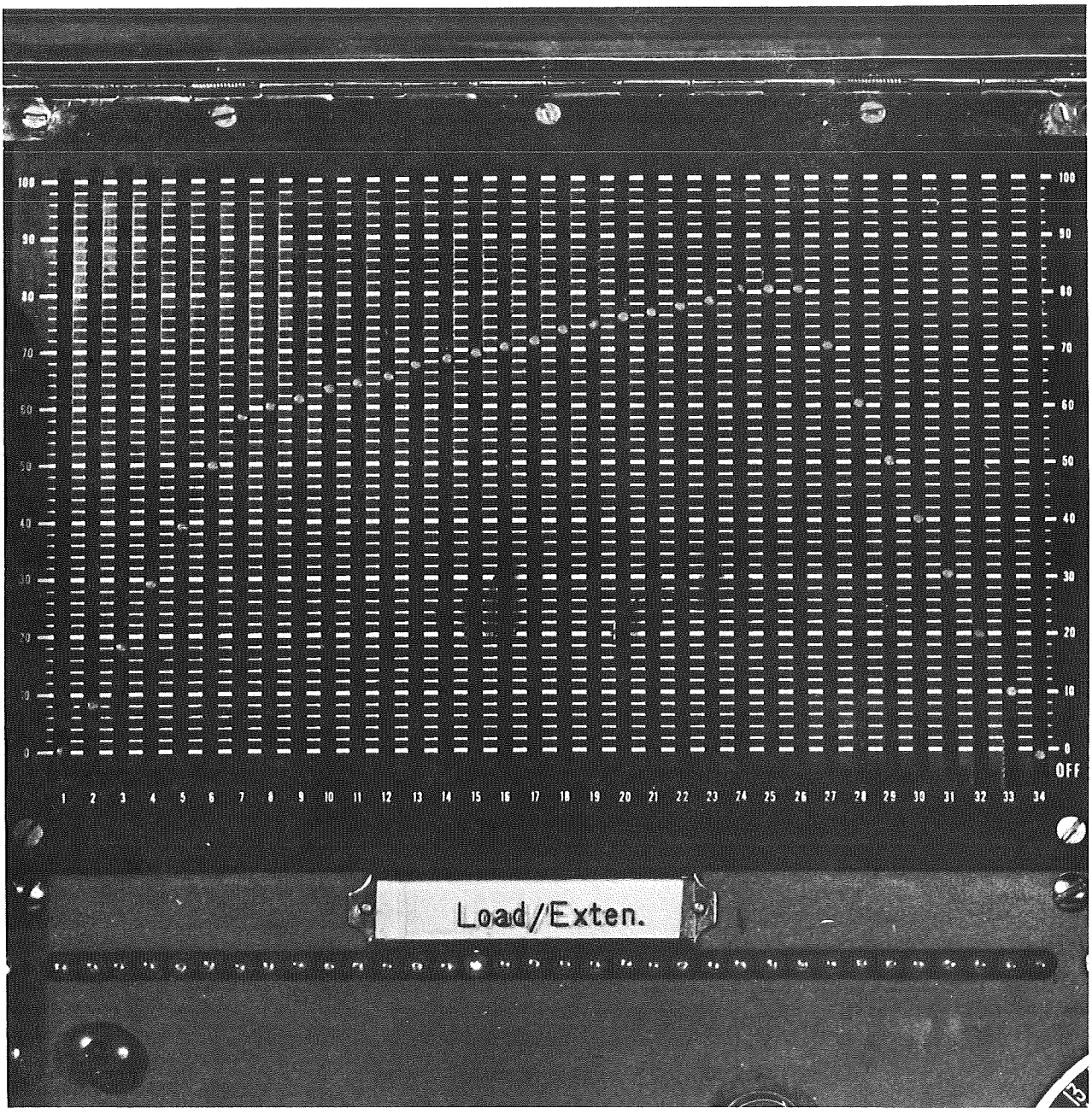

Figure V-6 Closeup View of Automatic Programer

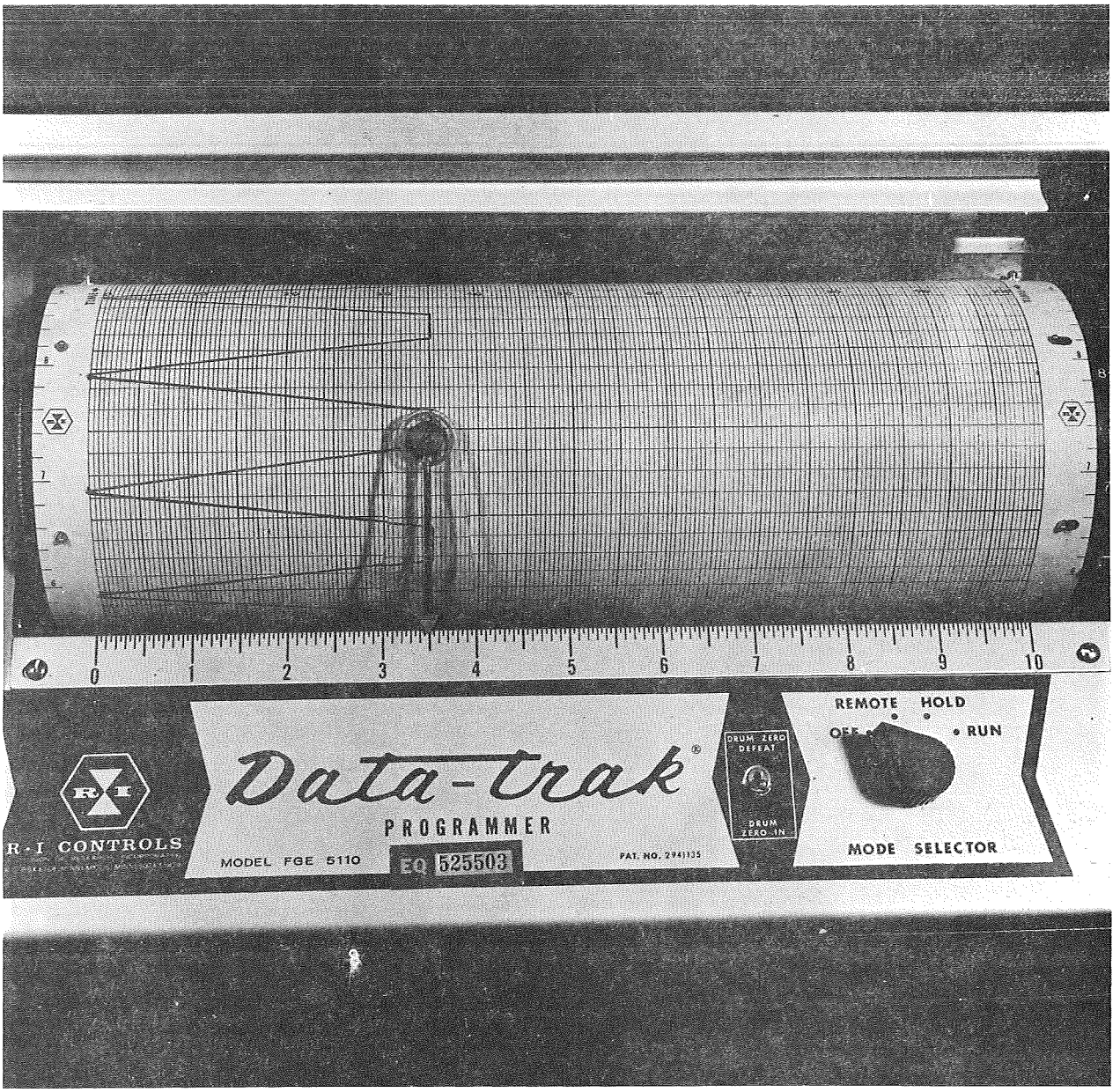

Figure V-7 Data Trak Programer

Two environmental chambers were designed and constructed for this work: One chamber was used at 70°F for the distilled water and 50% relative humidity air tests; a second unit was used for liquid nitrogen testing at -320°F. The room temperature chamber, shown in Figure V-8, was an air-tight aluminum box with plexiglass observation panels. The 50% relative humidity air environment was attained using a saturated aqueous solution of calcium nitrate, $Ca(NO_3) \cdot 4\ H_2O$, in the chamber. This solution, commonly used for humidity control, provides a 51% relative humidity at 24.5°C. Our experiments show that the chamber stabilized at a relative humidity of approximately 50% in 15 minutes. All air specimens were permitted to stabilize for 30 minutes prior to initiation of proof loading.

The cryogenic environmental chamber was a double walled stainless steel box approximately 2-inches thick containing poured polyurethane foam insulation. A single viewing port constructed from 1.5-inch thick acrylic plastic was installed to permit observation of the specimen during test. The lid was fabricated from 2-inch thick closed cell foam. Figure V-9 shows the cryogenic chamber.

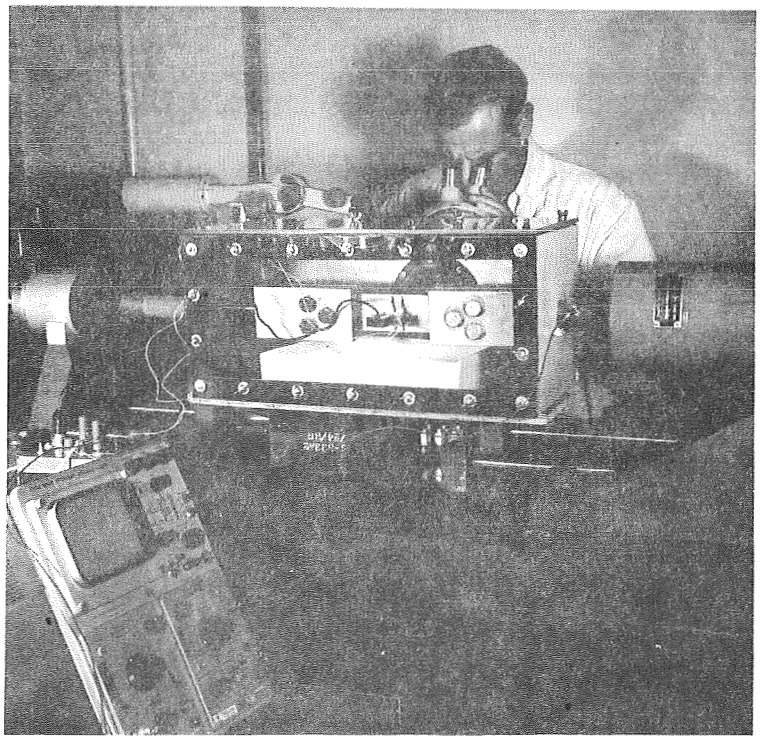

Figure V-8 Room Temperature Environmental Chamber

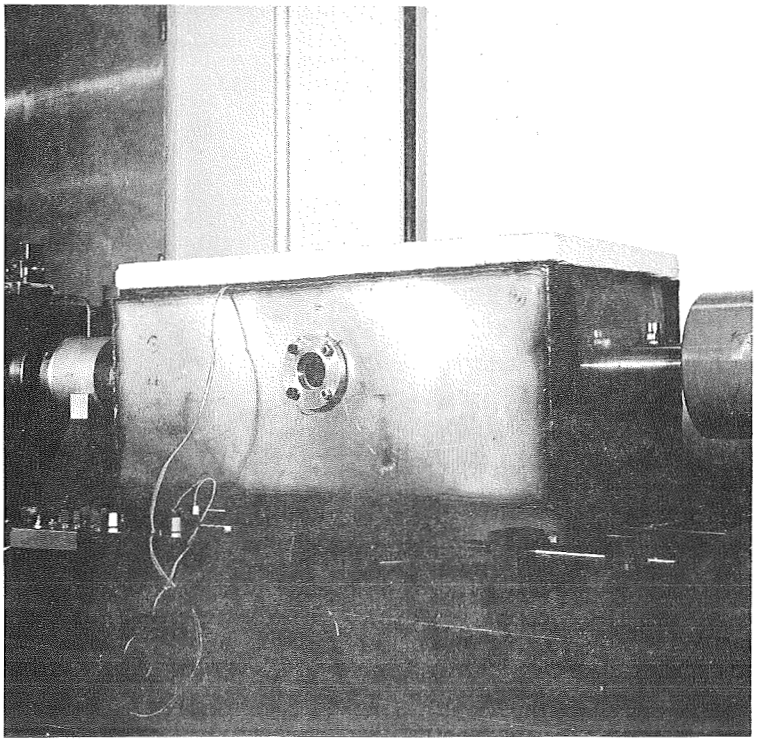

Figure V-9 Liquid Nitrogen Environmental Chamber

C. VISUAL EXAMINATION OF FRACTURE FACES

The fracture face of every specimen was visually examined for distinctive characteristics, i.e., initial flaw development, flaw growth during proof and cyclic growth limit. To help define each region of the flaw, specimens were exposed to a furnace oxidation cycle, one hour at 800°F after testing, to preferentially stain the defect surface. As a result of this oxidation cycle, the original fatigued flaw region turns to a gold color. The region of proof growth is also gold in color but has a distinct boundary between it and the original flaw.

Cyclic growth is very lightly stained and usually symmetrical about the proof boundary. The lighter oxidation of the cyclic growth area is to be expected since the crack front is propagating under smaller loads and the resulting crack is tighter. The proof cycle, in contrast, is a high stress condition causing a large crack opening displacement and relatively unhindered gas flow to this region. Keeping these flaw oxidation characteristics in mind, each specimen was examined using low magnification (about 30X) and the appropriate flaw measurements were obtained.

Comments regarding the extent of proof growth or the absence of it are noted in the proof test data tables in the Appendix. The magnitude of growth in the crack depth (a) and crack width (2c) directions are given. When the growth was greater at some other point on the periphery of the flaw, the magnitude of growth and the direction (ψ measured from semi-minor axis) are shown. In comparing the growth in the 0°(Δa), 90°(Δ2c), and ψ directions, it should be noted that in some cases the 90°(Δ2c) data appears to exhibit the greatest growth. It should be remembered that this value consists of growth at each end of the crack, and therefore one-half of this value should be compared with the growth in the other directions.

VI. EXPERIMENTAL DATA AND DISCUSSION OF RESULTS

Test data in either tabular or graphical form are summarized and the test results are discussed in this chapter. A guide to aid the reader in locating the data tabulated in the Appendix is given at the beginning of each section.

A. MECHANICAL PROPERTY TESTS

APPENDIX GUIDE - TENSILE PROPERTY TESTS

Description of Table	Table No.
70°F Tensile Properties	A-1
-320°F Tensile Properties	A-2

The tensile properties of the stress relieved 6Aℓ-4V STA titanium sheet material are summarized in Table VI-1. The parent metal ultimate strength level is approximately 1 to 3 percent lower than the as-heat-treated results reported in the vendor certification (Table IV-1). This slight reduction is a normal result of the stress relieving operation. Weld joint efficiency, approximately 90 percent, is typical for this alloy. Ductility at 70°F, almost 10 percent, was normal for the parent metal condition. No ductility measurements were taken at -320°F.

Table VI-1 Tensile Properties of 6Aℓ-4V STA Titanium

	70°F			-320°F	
CONDITION	ULTIMATE TENSILE STRENGTH (ksi)	YIELD STRENGTH 0.2% OFFSET (ksi)	ELONGATION (% in 2 in.)	ULTIMATE TENSILE STRENGTH (ksi)	YIELD STRENGTH 0.2 OFFSET (ksi)
0.090-in.					
Parent Metal	166.0	158.0	10.0	255.4	245.4
Weld Centerline	148.0	131.3	2.5	229.8	214.2
Heat Affected Zone	149.3	139.5	2.3	231.4	223.0
0.060-inch					
Parent Metal	168.0	159.5	8.5	255.7	245.7
Weld Centerline	154.9	130.1	2.7	246.0	217.5
Heat Affected Zone	154.3	147.3	2.5	243.6	229.1
0.030-inch					
Parent Metal	161.6	150.4	8.5	248.8	237.1
Weld Centerline	151.9	127.7	1.5	252.8	245.5
Heat Affected Zone	151.0	143.1	1.8	254.1	234.6

B. STATIC FRACTURE TOUGHNESS

APPENDIX GUIDE - STATIC FRACTURE TOUGHNESS	
DESCRIPTION OF TABLE	TABLE NO.
0.090-inch; 70°F	A-3
0.060-inch; 70°F	A-4
0.030-inch; 70°F	A-5
0.090-inch; -320°F	A-6
0.060-inch; -320°F	A-7
0.030-inch; -320°F	A-8

Static fracture toughness properties are summarized in Table VI-2. In order to obtain satisfactory average properties, a significant number of static tests had to be performed. The results of almost 60 tests are reported. At 70°F, the range of fracture toughness values was sufficiently small so that a satisfactory average could be obtained. However, at -320°F a moderate spread was obtained; although the range of toughness was moderate, average properties were calculated for use in proof test calculations. At 70°F, it appears that the fracture toughness level is a function of fracture/yield strength ratio. Although some slow flaw growth occurred during the static toughness tests, no instrumentation was used that would have detected the stress at which growth initiated. The range of toughness values for the 0.090-inch material was fairly limited and data for this thickness did not require magnification $\left(M_K\right)$ correction. The 0.060-inch results also exhibited small data scatter. Although the crack depth thickness (a/t) ratio was great, the crack shape (a/2c) ratio was sufficiently high that the need for magnification ratio appeared unnecessary. The 0.030-inch stock also showed limited data scatter. For these specimens, an M_K correction could be utilized. However, because there is still some uncertainty as to the magnitude of the elastic magnification factors, and, in addition, the effects of plasticity have still not been assessed, it was decided not to incorporate M_K correction.

Table VI-2. Static Fracture Toughness Properties of 6Aℓ-4V STA Titanium

TEMPERATURE (°F)	THICKNESS (in.)	LOCATION	FRACTURE TOUGHNESS K_{Ic} (ksi$\sqrt{in.}$)
70	0.090	PM	50.8
		WC	53.4
		HAZ	50.6
70	0.060	PM	47.2
		WC	48.2
		HAZ	47.6
70	0.030	PM	39.6
		WC	34.9
		HAZ	33.1
-320	0.090	PM	48.7
		WC	59.6
		HAZ	55.1
-320	0.060	PM	46.0
		WC	51.2
		HAZ	47.5
-320	0.030	PM	41.0
		WC	40.7
		HAZ	36.6

Note: PM = parent metal;
WC = weld centerline;
HAZ = heat affected zone.

The liquid nitrogen (-320°F) tests showed a moderate data spread. As for the 70°F, the 0.090 and 0.060-inch material did not appear to require M_K correction. An evaluation of stress versus crack size (σ vs a/Q) showed an interesting effect. By plotting the data, we see a tendency for the larger crack sizes to exhibit the lower toughness values. These lower bound values are representative of the toughness based on the initial flaw size and the final fracture stress. Since no instrumentation was utilized on the static tests, the stress at which slow flaw growth initiated could not be detected. It is assumed that the larger flaws may have an increased tendency to slow growth and, as a result, give the lower bound values. Figure VI-1 gives the stress versus crack size plots for the 0.090-inch titanium. The 0.090-inch weld centerline data show toughness significantly greater than the parent metal and heat affected zone. No reason is apparent for the high toughness obtained in some tests performed on weld centerline specimens.

The 0.060-inch titanium tested at -320°F showed behavior quite similar to the 0.090-inch material. Examination of the data indicate that the isolated low toughness values are associated with the lowest a/2c ratios and largest crack depths; this combination tives the largest crack area and tends to substantiate the concept that the tendency toward slow flaw growth is greatest for the largest crack sizes. In one case, specimen 6W4-7, the low toughness was associated with a very coarse grained portion of the weld zone.

The 0.030-inch specimens generally had a low a/2c ratio and crack depths exceeding 50 percent. This combination should require magnification correction, but for the reasons previously described no correction was attempted.

C. PROOF TESTS

APPENDIX GUIDE - PROOF TESTS	
Description of Table	Table No.
0.090-inch; air	A-9
0.090-inch; water	A-10
0.090-inch; LN_2	A-11
0.060-inch; air	A-12
0.060-inch; water	A-13
0.060-inch; LN_2	A-14
0.030-inch; air	A-15
0.030-inch; water	A-16
0.030-inch; LN_2	A-1-

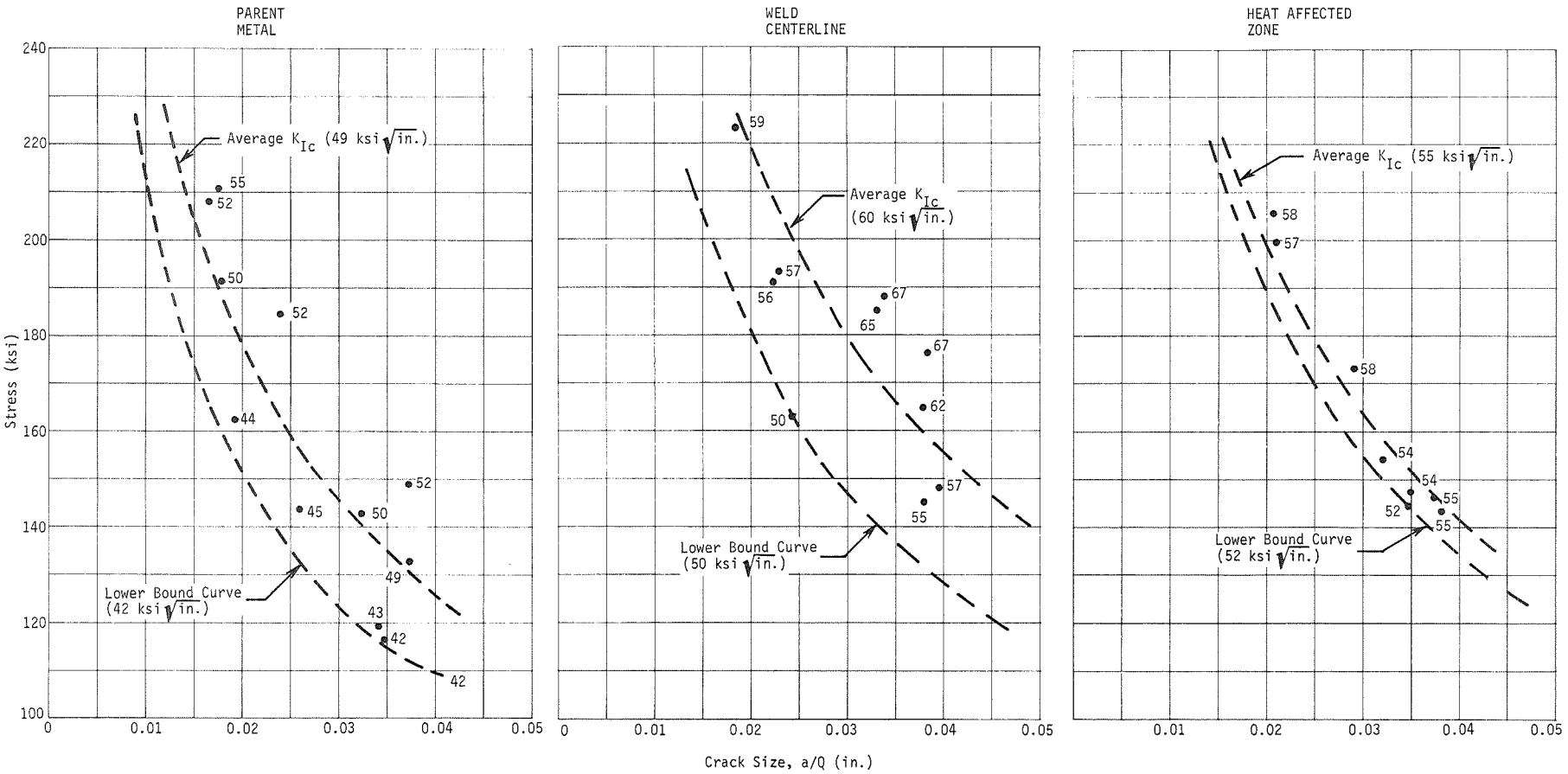

Figure VI-1 Stress versus Crack Size Curves for 0.090-inch 6Al-4V Titanium

Proof test exposure data are summarized in Table VI-3. Examination of this table shows that slow flaw growth does occur during proof testing. It is further noted that pop-in behavior occurred infrequently. Tunneling behavior occurred in some cases. In most cases, the level at which slow growth was detected exceeded 85% of the critical stress intensity level.

In the following paragraphs more detailed observations on proof test exposures are discussed.

1. 0.090-inch Titanium/Air

Tests performed in air showed slow growth in all cases. The strain gage and compliance gages were quite successful in detecting the initiation of slow growth. This was noted as an abrupt step in the load versus strain or displacement curve. Since the plotters were being continually observed during the test, we were able to ascertain that the crack growth that caused the step occurred in a slow fashion. If pop-in had occurred, the step would have been plotted instantly. In addition, an audible pop and accelerometer indication would have been obtained.

The parent metal-air tests showed tunneling in one case. This specimen exhibited a high a/2c ratio. Two failures during proof occurred at a stress intensity in excess of 100% of the average critical stress intensity. The magnitude of crack growth was quite small (less than 0.003 in.).

In the weld centerline tests, one specimen cracked through to the backface during proof but did not fail; no proof failures occurred for the weld centerline. The magnitude of growth was generally small (several thousands of an inch).

Tests of the heat affected zone showed the greatest amount of flaw growth. One specimen exhibited 0.006-inch growth in the semi-minor axis direction. Three tests resulted in failure during proof; in all cases, the applied stress intensity exceeded 100% of the average K_{Ic}.

2. 0.090-inch Titanium/Water

The parent metal tests conducted in distilled water showed slow growth in all cases. Tunneling was found in a 0.4 a/2c ratio shaped crack. Figure VI-2 shows the fracture face of this specimen; arrows show the extent of tunneling.

Table VI-3 Summary of Proof Test Results

THICKNESS (in.)	LOCATION	AIR			WATER			LIQUID NITROGEN		
		TYPE OF GROWTH	DETECTION LEVEL, % K_{Ic}	GROWTH DESCRIPTION	TYPE OF GROWTH	DETECTION LEVEL, % K_{Ic}	GROWTH DESCRIPTION	TYPE OF GROWTH	DETECTION LEVEL, % K_{Ic}	GROWTH DESCRIPTION
0.090	PM	Slow	0.91-0.94	T, U, NU, NV	Slow	0.90-0.95	T, U	Slow	NI	U, NU, NV
	WC	Slow	0.86-0.91	U, NU, NV	Slow	0.90-0.95	NU	Slow	0.82	U, NU, NV
	HAZ	Slow	0.91-0.96	U, NU, NV	Slow	0.78-0.94	U, NU	Slow	NI	NU, NV
0.060	PM	Slow	0.88-0.95	T, U, NU	Slow	0.89-0.98	T, NU	Slow	NI	U, NU, T
	WC	Slow	0.89-0.98	U, NU	Slow	0.92-0.94	U, NU, NV	Slow	NI	NU
	HAZ	Slow	0.91-0.94	U, NU	Slow	0.83-0.88	NU, NV	Slow	NI	U, NU, NV
0.030	PM	Slow	0.85	NU, NV	Slow	0.92	NU, NV	Slow	0.89	U, NU
	WC	Slow	0.94-0.95	NU, NV	Slow	0.93	NU	Slow	NI	NU, NV
	HAZ	Slow	0.88	NU, NV	Slow	0.92	NU, NV	None	NI	NV

Code: PM - parent metal
WC - weld centerline
HAZ - heat affected zone

T - tunneling
U - uniform flow growth
NU - nonuniform

UV - no visible growth indication
NI - no indication

The remainder of the specimens showed uniform slow growth of approximately 0.003-inch. Weld centerline specimens showed slow nonuniform growth; however, the magnitude of growth was quite small, as in the case of the parent metal. A typical fracture face is shown in Figure VI-3; arrows show the extent of the slow nonuniform growth.

The heat affected zone specimens showed a slight amount of growth. A typical example is shown in Fig. VI-4.

3. 0.090-inch Titanium/Liquid Nitrogen

Parent metal specimens tested in liquid nitrogen showed very small amounts of slow growth (Fig. VI-5). Three specimens failed during proof; however, no correlation to percentage of K_{Ic} could be established to explain the proof failures. Because of the small cracks used at LN_2 temperature (Cracks were small because of the higher nominal proof stress.), it is almost impossible to detect the level at which slow crack growth initiated. The little growth that occurred was generally nonuniform.

Weld centerline tests also showed very little growth. Analysis of the actual K_{Ii}/K_{Ic} ratio showed that we were on the low side of the desired range; most tests were approximately 90% K_{Ic}. An indication of the initiation level was found for one specimen at 82% K_{Ic}. However, in view of the small flaw size and single test result, it is difficult to place great confidence on this test result. Visual observation of the fracture faces showed the growth to be generally nonuniform.

Evaluation of the heat affected zone tests showed that no proof failures occurred even though the applied stress intensity was as high at 106% K_{Ic}. Two specimens (96 and 106% K_{Ic}) showed visible growth (although small); no indications from our instrumentation were obtained for these tests. The remainder of the specimens showed no visible flaw growth. It should be noted that visual evaluation to detect flaw growth is quite difficult for the weld and heat affected zone regions, particularly for the small size liquid nitrogen defects.

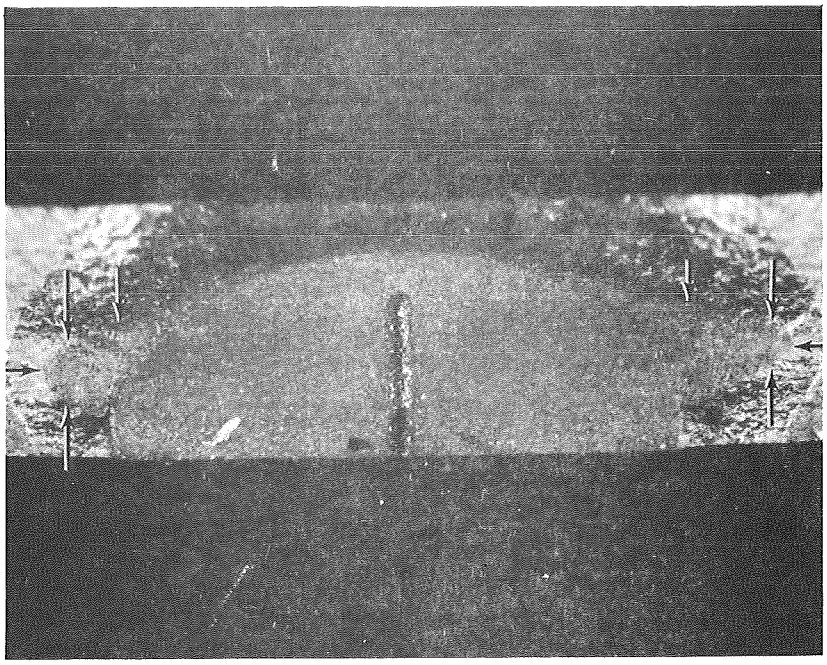

Figure VI-2 Fracture Face of Specimen Showing Tunneling Behavior (specimen 9CP-7; 0.090-inch; water; arrows show extent of tunneling)

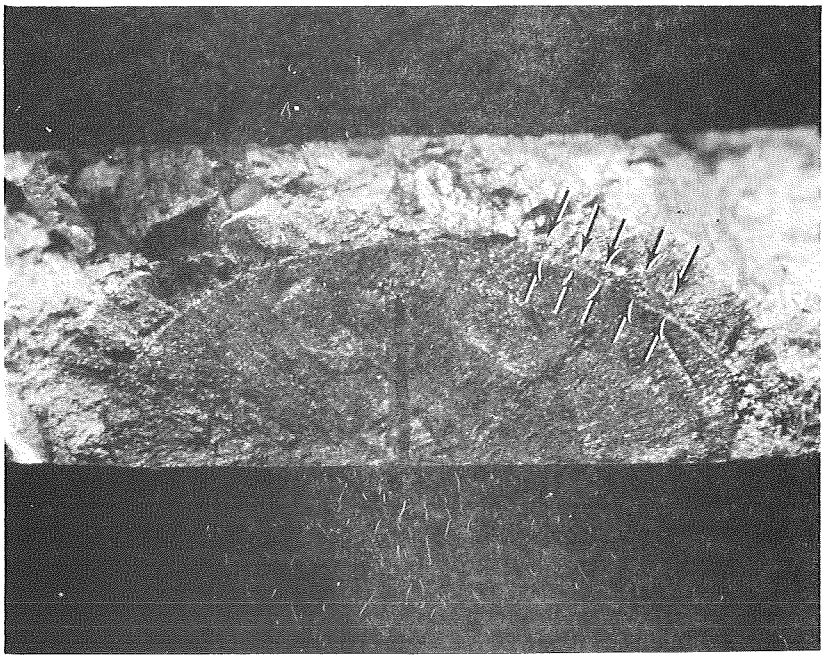

Figure VI-3 Fracture Face of Specimen Showing Nonuniform Flaw Growth in Weld Centerline (specimen 9W3-3; 0.090-inch; water)

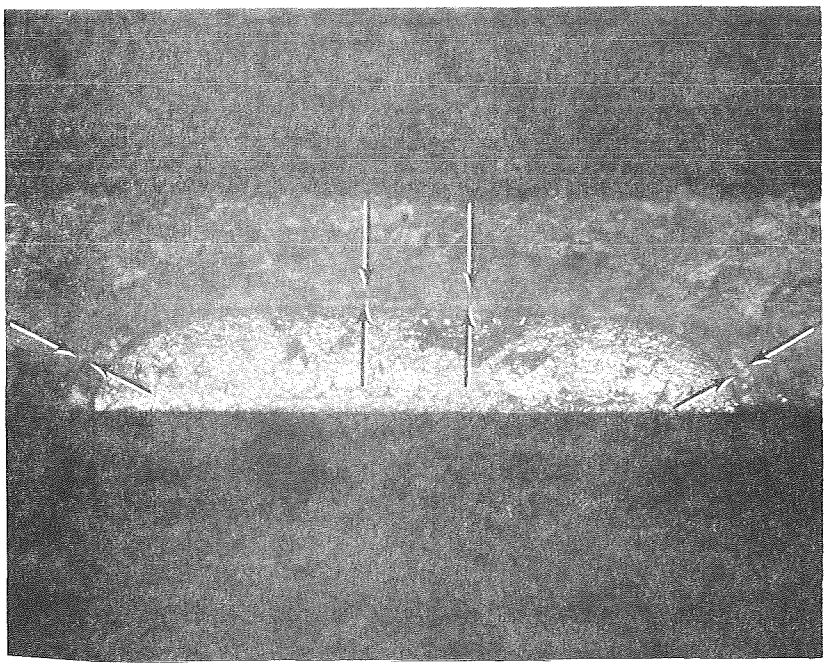

Figure VI-4 Fracture Face of Specimen Showing Slight Uniform Flaw Growth (specimen 9W9-1; 0.090-inch; water)

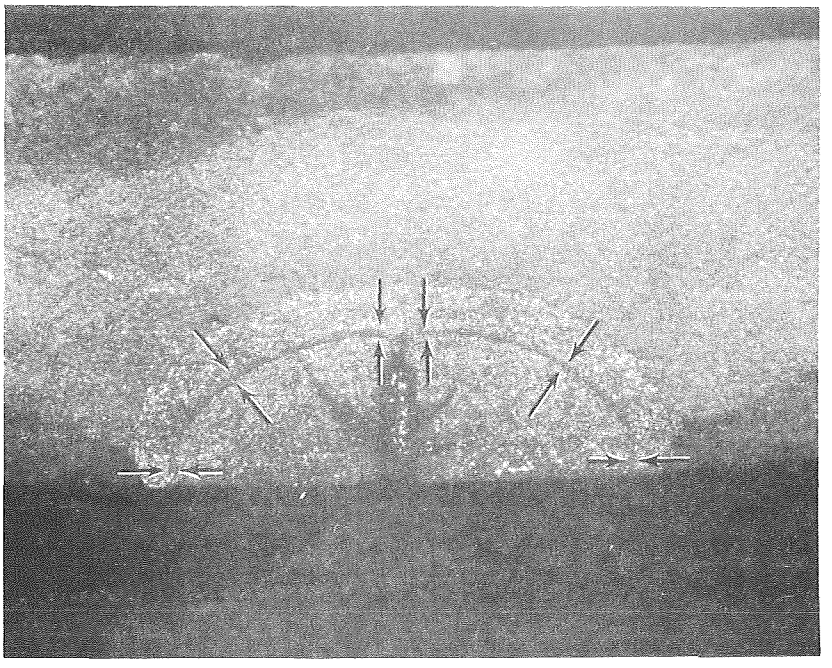

Figure VI-5 Fracture Face of Specimen Showing Small Uniform Growth (specimen 9CP-45; 0.090-inch; LN_2)

4. 0.090-inch Titanium/Summary

All growth in the 0.090-inch specimens was of the slow type. Growth appeared to be greater in the heat affected zone at 70°F. No great difference between air and water testing was found. Tunneling behavior appears to occur with greater ease for the higher a/2c ratios. Flaw growth at -320°F was quite minor.

5. 0.060-inch Titanium/Air

All crack growth was of the slow type. Figure VI-6 shows a typical example of slow growth around the crack front with a small tendency to square off. No pop-in was detected. Some tunneling growth was observed in the parent metal. Although some parent specimens were loaded to a high stress intensity (108%), no proof failures occurred. During the 30 minute hold period, growth up to 0.006 inch was found.

Weld centerline tests showed failure of two tests that had been subject to the highest stress intensities. Crack growth for these specimens was up to 0.003 inch. The remainder of the specimens exhibited nonuniform growth. Heat affected zone specimens exhibited up to 0.003-inch flaw growth.

6. 0.060-inch Titanium/Water

Two parent metal specimens exhibited failure during the proof test. Both of these tests were performed at high stress intensities. Another specimen exhibited tunneling behavior but did not fail; no evidence of pop-in was found. Short time hold specimens showed less than 0.004-inch flaw growth.

One 30-minute hold specimen exhibited tunneling behavior (Fig. VI-7). Crack growth for the long time hold specimens was 0.002 to 0.005 inches.

Weld centerline tests showed growth during short time hold. Two specimens failed during proof; these were loaded to high stress intensity levels.

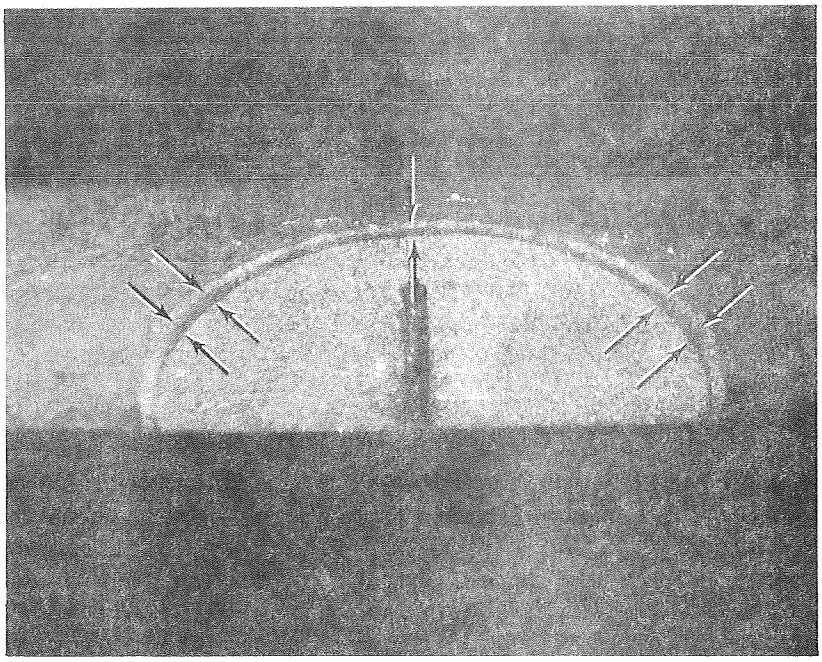

Figure VI-6 Fracture Face of Specimen Showing Tendency to Square Off (specimen 6CP-3; 0.060-inch; air)

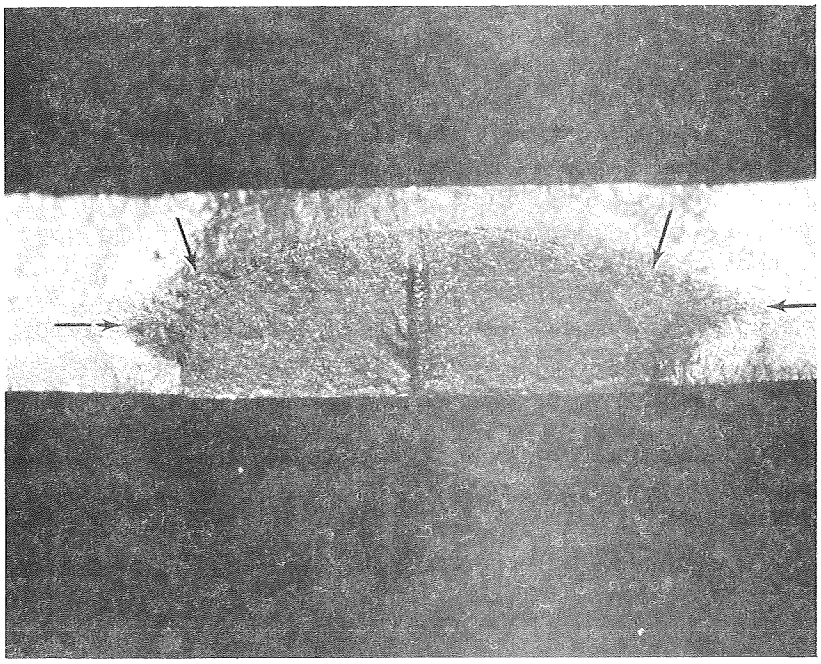

Figure VI-7 Fracture Face of Specimen Showing Tunneling Behavior (specimen 6DP-4; 0.060-inch; water)

The heat affected zone tests were characterized by an apparent lower level for the initiation of flaw growth. However, since this was found only by a single test, the validity of the result should be confirmed by additional work. Proof failures occurred in three out of five tests. Growth was principally nonuniform.

7. 0.060-inch Titanium/LN_2

Parent metal specimens exhibited slow flaw growth. Although an audible indication was found in one test, no confirmation of pop-in could be established. No accelerometer indication was obtained because of excessive background noise in the liquid nitrogen environmental chamber.

Many of the specimens failed during proof testing. Growth was limited; uniform growth generally did not exceed 0.002 inch.

Weld centerline specimens showed slow growth; no pop-in was observed. Most specimens failed during proof. A moderate amount of growth (up to 0.005 inch) was observed for these specimens.

Heat affected zone tests all showed slow growth of a very limited nature.

8. 0.060-inch Titanium/Summary

Tunneling was found in some parent metal specimens. On the basis of the available data, it was not possible to correlate the tendency for tunneling to crack size or shape. Actually very few specimens exhibited pop-in behavior. Tunneling was found for all three environments. The magnitude of parent metal growth was modest at 70 and -320°F.

Weld centerline and heat affected zone specimens exhibited minimal growth at both 70 and -320°F. Growth was slow with no evidence of tunneling. No significant differences in the magnitude of growth for the three defect locations, other than tunneling in the parent metal, were noted.

9. 0.030-inch Titanium/Air

One parent metal test failed at 100% K_{Ic}; a second cracked through at 103% K_{Ic} but did not fail. These tests serve to illustrate that fracture is quite marginal under the conditions evaluated. The amount of flaw growth was rather small; at 90%K_{Ic}, no visible growth was found.

Weld centerline tests showed failures above 100% of average K_{Ic}. The actual amount of flaw growth was difficult to ascertain because most tests resulted in proof failure.

Examination of the heat affected zone tests showed that two specimens failed; a third did not show visible growth. It was difficult to determine the magnitude of slow growth.

No pop-in was found for any of the three defect locations.

10. 0.030-inch Titanium/Water

Parent metal tests exhibited slight growth. At 104% K_{Ic} a small amount of nonuniform growth was observed. At 94% K_{Ic}, no visible indications of growth were found.

Weld centerline tests showed slight growth; one specimen failed at 99% K_{Ic}.

The heat affected zone group showed tunneling in a single specimen at 104% K_{Ic}. Another specimen tested at 106% K_{Ic} showed no visible indications of crack growth.

11. 0.030-inch Titanium/Liquid Nitrogen

Parent metal specimens showed slow flaw growth of a limited magnitude. One specimen exhibited 0.006 inch of slow growth.

Weld centerline specimens showed only slow growth. The magnitude of growth was very modest.

Specimens containing defects in the heat affected zone showed very limited growth of the slow type.

12. 0.030-inch Titanium/Summary

All specimens that exhibited growth, grew in a slow manner. Tunneling did not appear to be a factor in the 0.030-inch stock. It was difficult to determine the magnitude of the slow growth because some of the specimens failed during proof; however, it appeared that the amount of growth was very limited and normally nonuniform around the crack front.

D. CYCLIC TESTS

APPENDIX GUIDE - CYCLIC TESTS	
Description of Table	Table No.
0.090-inch	A-18
0.060-inch	A-19
0.030-inch	A-20

Cyclic tests were performed for all specimens that passed the proof test without failure. The objective of the cyclic testing was to determine (1) crack growth rate data, (2) susceptibility toward failure at a reduced stress after passing the proof test, and (3) whether defects that exhibited tunneling showed more growth than would be predicted for more normal shaped semielliptical cracks.

Graphical presentations of the data are given in Figures VI-8 through 10. For the 0.090-inch material, parent metal appears to be somewhat more resistant to growth than weld centerline or heat affected zone stock. For the thinner gages, this effect is less pronounced. The 0.030-inch titanium shows almost identical rate data for the heat affected zone and weld centerline; parent metal data can be plotted as a parallel line without slightly less sensitivity toward growth.

The graphical presentation of cyclic growth data show points with arrows leading to the right in many cases. These points represent those conditions where the average crack growth rate was reduced by the proximity of the backface. These points normally fall above the average curve.

In order to ascertain the susceptibility toward brittle fracture at reduced stress following the proof test, and approximate analysis must be performed. First, it should be noted that in performing the cyclic tests we attempted to satisfy two competing goals. The first was to obtain cyclic growth rate data using the linear interpolation technique; in order to do this, the amount of crack extension must be minimized so that the initial and final stress intensities are as similar as possible. In order to evaluate the susceptibility to fracturing, the maximum amount of crack extension must be obtained. In our work, we compromised by performing limited extension and large extension tests. As a result of analyzing the data for those tests that failed or were discontinued at less than the 500-cycle maximum because failure was imminent, we can reasonably well categorize the stress intensity level above which failure is likely in 500 cycles at a maximum cyclic stress of 105 ksi. These approximate levels are tabulated:

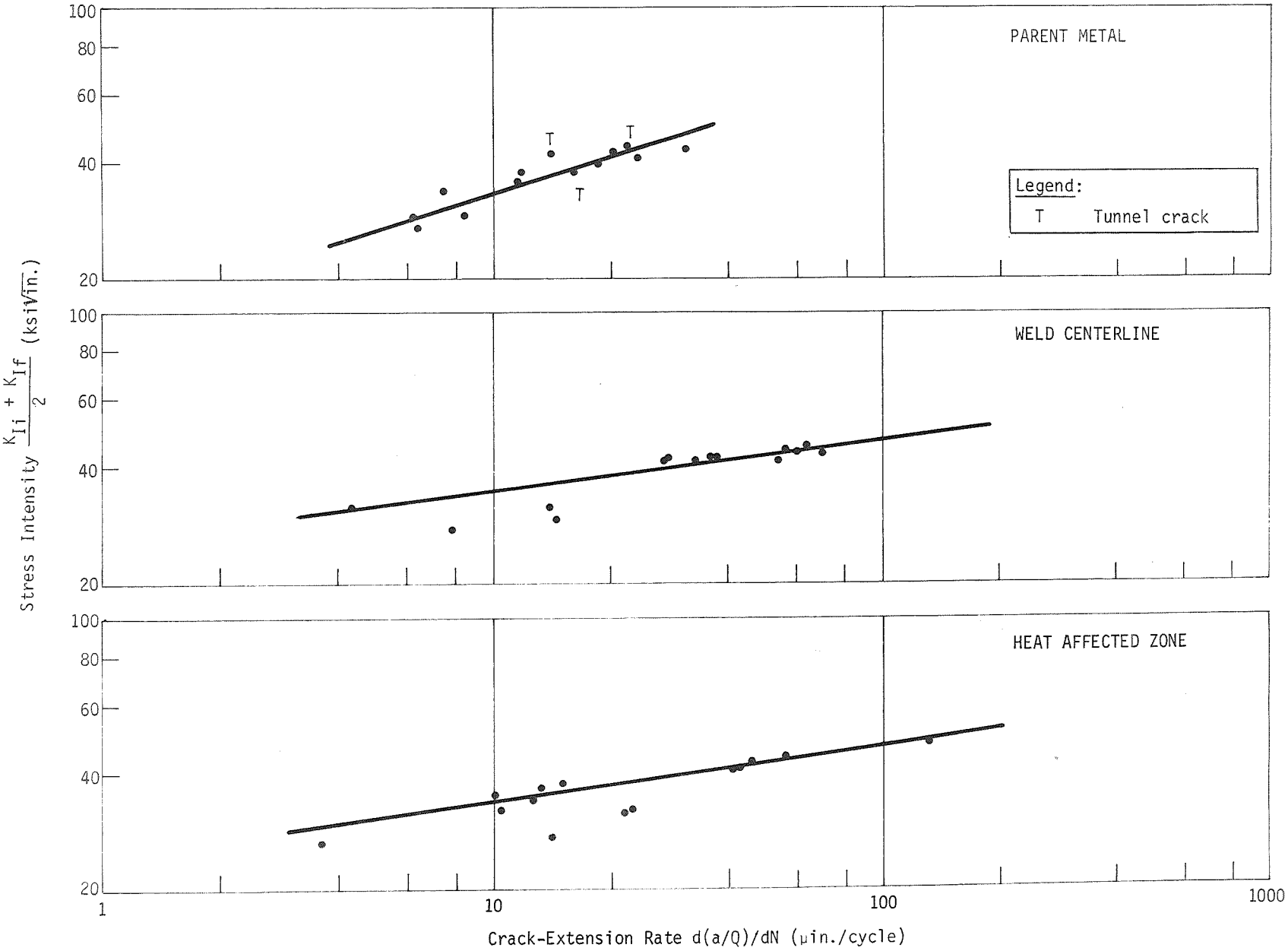

Figure VI-8 Cycle Crack-Extension Rates for 0.090-inch 6Aℓ-4V Titanium

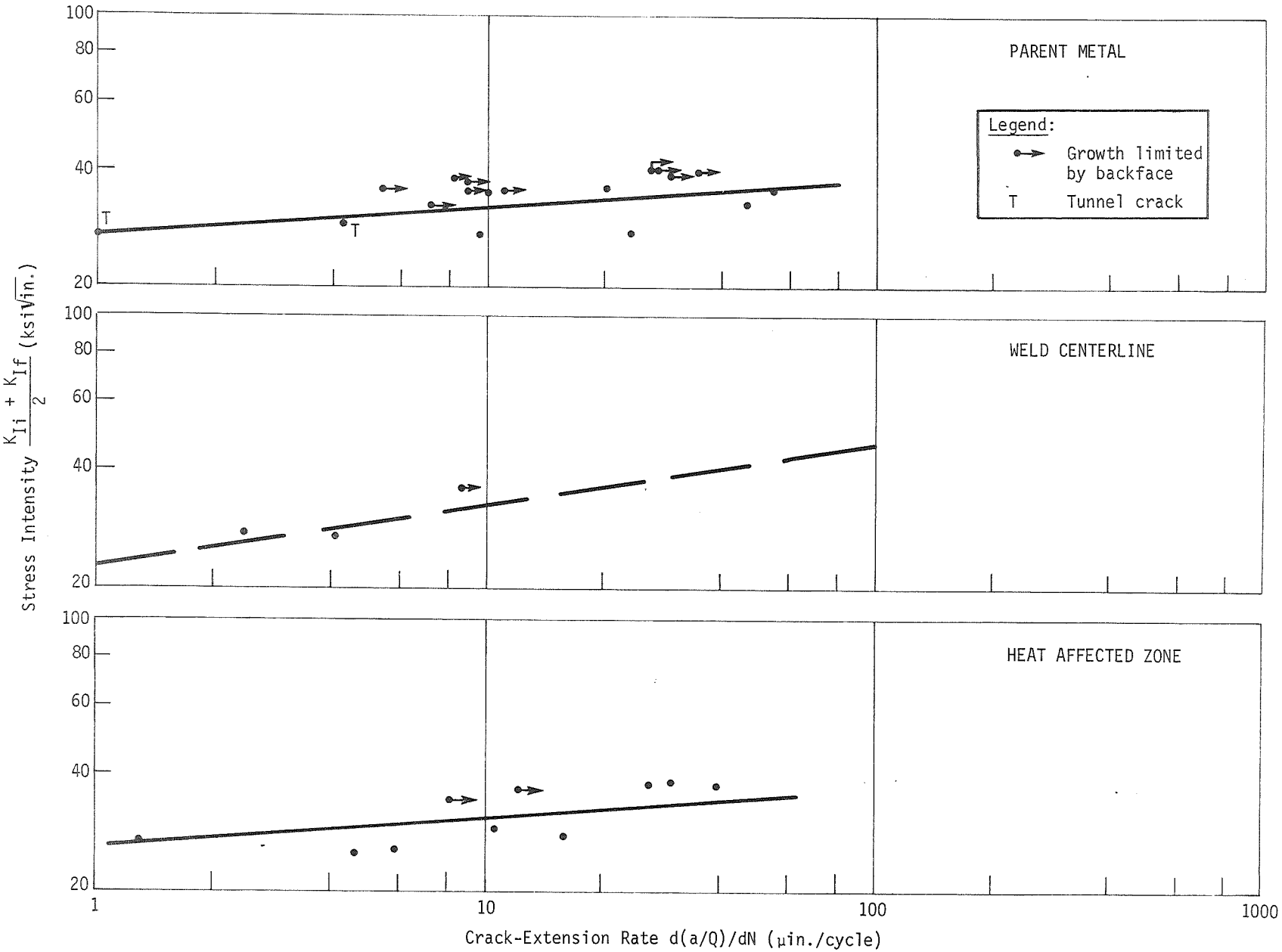

Figure VI-9 Cyclic Crack-Extension Rates for 0.060-inch 6Aℓ-4V Titanium

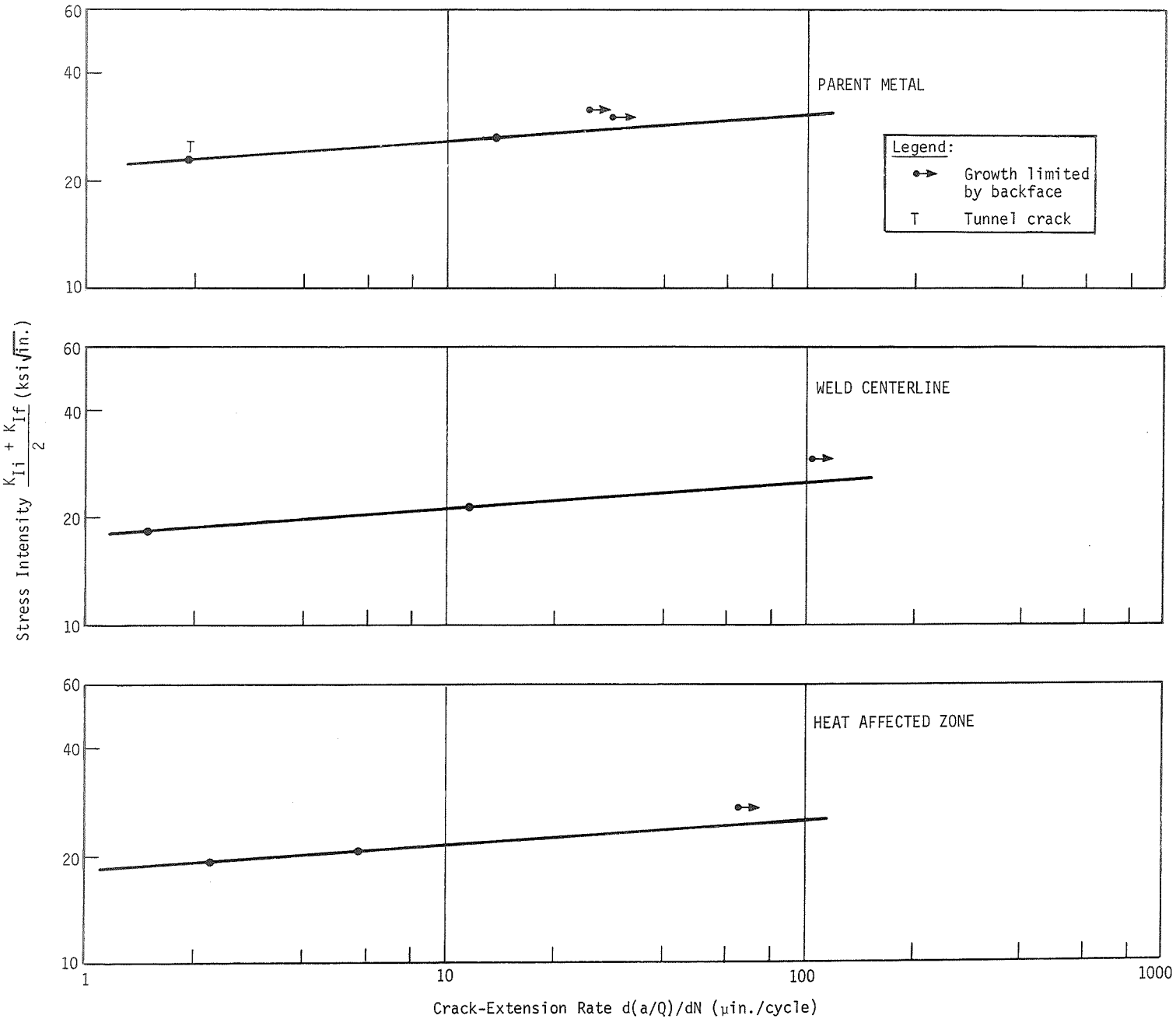

Figure VI-10 Cyclic Crack-Extension Rates for 0.030-inch 6Aℓ-4V Titanium

THICKNESS (in.)	LOCATION	STRESS INTENSITY, K_{Ii} (ksi $\sqrt{in.}$)
0.090	PM	44
	WC	42
	HAZ	40
0.060	PM	38
	WC	35
	HAZ	35
0.030	PM	27
	WC	25
	HAZ	25

PM = parent metal;
WC = weld centerline;
HAZ = heat affected zone.

The effect of tunneling on crack growth is somewhat difficult to handle unless we make some simplifying assumptions. Although the tunnel shaped crack is not semielliptical, if we handle it as though it were semielliptical in order to calculate stress intensity, we then have a situation where the calculated stress intensith is probably on the low side. If this is true, the crack extension data should then be abnormally high when compared with semielliptical data. Therefore, we can handle the analysis best in a graphical fashion by identifying the tunnel shaped cracks and observing whether these fell below the average curve. It was anticipated that no significant effect would be noted because those cracks where tunneling was noted did not show deep tunneling; actually the effect of tunneling on the crack width (2c) dimension was not great. In some cases, the tunneling effect was merely to square off the crack. Recognizing modest changes in crack width as small contributions to the flaw shape parameter (Q), it would not be surprising if no effect were noted. Examination of the graphical presentations shows no significant effect.

Fracture toughness properties were determined on specimens after cyclic loading. In general, these data were not sufficiently valid to permit reporting. The principal reasons were excessively deep final crack size, possible damage due to heat tinting, and, for some liquid nitrogen sepcimens, the crack size was too small to obtain fracturing below the yield strength.

VII. ANALYTICAL TECHNIQUES

A. STRESS INTENSITY FOR SURFACE-FLAWED SPECIMENS

Irwin (Ref 6) has estimated the effect of shape on stress intensity in a semielliptical surface flaw subject to a normal load by using the following equation:

$$K_I = \frac{M_1 \sqrt{\pi a}\, \sigma \left(\sin^2 \phi + \frac{a^2}{c^2} \cos^2 \phi\right)^{1/4}}{\left[\Phi^2 - 0.212 \left(\frac{\sigma}{\sigma_{ys}}\right)^2\right]^{1/2}}$$

where:

M_1 is a free-surface correction factor generally taken as 1.1;

σ is the applied tensile stress;

a is the length of the semiminor axis;

ϕ is the angle between the major axis and any point on the flaw front;

c is the length of the semimajor axis;

Φ is the complete elliptical integral of the second kind and may be expressed by:

$$\Phi = \int_0^{\pi/2} \sqrt{1 - \frac{c^2 - a^2}{c^2} \sin^2 \phi}\; d\phi.$$

The term $\left[\Phi^2 - 0.212 \left(\frac{\sigma}{\sigma_{ys}}\right)^2\right]$ is commonly called Q. By letting ϕ = 90 deg the limiting equation for stress intensity can be expressed as:

$$K_I = 1.1 \sqrt{\pi}\, \sigma \left(\frac{a}{Q}\right)^{1/2}.$$

Several modifications have been made to the above approximate solutions in order to account for the effect of the proximity of the back face. These have been reported by Kobayashi (Ref 7) and Smith (Ref 8). Recent experiments performed by Larson (Ref 9) and Smith (Ref 10) using cast epoxy specimens indicate that the back-surface correction factors are approximately 20 to 25% lower than those predicted by Smith (Ref 8).

In this work, attempts were made to avoid making cracks deep enough to require back-surface correction of the stress-intensity factor. However, because of the thin gages and the necessity to utilize specific proof stresses this was not always possible. Back-surface correction factors were not used because there is still some uncertainty as to the magnitude of the elastic magnification factors, and in addition, the effects of plasticity have still not been assessed.

B. CYCLIC FLAW GROWTH

During cyclic loading, a small amount of growth is considered to have occurred during each load cycle. If the increment of crack extension that occurs during a specific number of cycles can be determined, it is possible to prepare a crack extension curve of crack length (a) vs number of cycles (N). The slope of the curve at any point is the crack growth rate (da/dN). From an experimental standpoint, this technique is relatively simple to apply for through-cracked specimens. However, for semielliptical surface-flawed specimens this is not readily accomplished because the critical crack parameter, the crack depth, is not visually measurable from the surface. Because the shape of the crack usually changes as the crack grows in depth, determining the crack width, which is readily discernible on the surface, does not provide quantitative information.

Boeing (Ref 11 and 12) has evaluated flaw-growth behavior in surface-flawed specimens using the "end point analysis" method. In this method, the initial stress intensity $\left(K_{Ii}\right)$ is plotted against the number of cycles to failure, and these data are converted to an initial crack size (a/Q) vs N curve at a given stress. From this curve, the slope or crack growth rate [d(a/Q)/dN] can be obtained for a specific a/Q. The latter can be converted to a value of K_I at a given stress, and as a result, a stress intensity vs growth rate curve can be obtained.

This method is dependent on several factors:

1) The specimen must be taken to fracture;
2) The critical crack depth must be sufficiently less than the thickness to avoid plasticity effects;
3) The critical crack size must be distinguishable from the rapid fracture;
4) A semielliptical shape must be maintained.

Satisfying these criteria gives a simple method for determining crack growth. However, it is necessary for the test to be conducted until failure occurs.

Another method, used in this program, can be called the "linear interpolation" technique. This approach is to minimize the amount of flaw growth, thereby making the initial and final stress intensities similar enough so that a rate based on the initial and final crack sizes is a valid linear interpolation of the slope of the crack size vs number of cycles curve. It is important to make a small linear interpolation because the error that can result in a power function relationship, in this case one theorized to be a fourth power relationship, can be quite significant.

VIII. CONCLUSIONS

Based on the data generated in the performance of this program, the three objectives of this research have been satisfied. These objectives were:

1) To determine whether flaw growth occurrence during proof testing results from environmental effects (e.g., slow growth caused by stress corrosion) or results from pop-in where the crack extends initially in a state of plane strain and is arrested when the state changes to plane stress;

2) To determine the effect of stress-intensity-factor level, plate thickness, flaw shape, flaw location, and environment on the occurrence of flaw growth during proof testing;

3) To determine the effect of flaw growth during proof testing on the remaining cyclic life at normal operating stress levels.

Flaw growth during proof testing is of the slow growth type. Although the occurrence of slow flaw growth implies a stress corrosion mechanism, our data does not indicate a sufficient difference in the susceptibility to slow growth to firmly show an environmental effect in comparing the various media. An analysis of stress intensity versus growth during proof showed the effect of hold time (30 minutes hold time resulted in more growth than 15 second hold time) but did not clearly differentiate between air and water exposures.

Tunneling behavior, as described in prior work by others, was neither prevalent nor significant. The magnitude of tunneling was not great; in most cases it was manifest by little more than a tendency to square off the semielliptical-shaped precrack. Tunneling behavior, under slow growth conditions, appears to be more prevalent with a high a/2c ratio in the gages tested. This is understandable because the cracks with a high a/2c ratio were rather deep in order to achieve the required stress and stress intensity combination. As a result, it is likely that the nose of the crack (end of semiminor axis) was subject to plasticity effects. Under these conditions, it is reasonable for growth to occur preferentially at some angle from the semiminor axis, thereby resulting in tunneling or squaring off behavior.

It was determined that the level at which flaw growth initiated was 85 to 90% of the critical stress intensity $\left(K_{Ic}\right)$. In a few cases, isolated test results indicated a somewhat lower initiation level; however, these lower levels occurred in welded material where crack propagation along certain preferred grain orientations has been observed.

At 70°F, slow growth was significant at high percentages of K_{Ic} and under longtime holding. Cryogenic tests showed that growth was quite minor at similar levels of stress intensity. This observation has caused us to conclude that the susceptibility to slow growth is strongly influenced by crack size, since the LN_2 specimens contained small flaws and did not exhibit great growth.

This conclusion is further substantiated by the results of our static fracture toughness tests where the specimens with the largest flaws exhibited below-average toughness, suggesting that a lower bound value based on the product of initial flaw size and fracture stress was actually determined.

Parent metal material exhibited the greatest resistance to flaw growth for all gages and environments. The least resistance to flow growth was found for the 0.090-inch material in the heat affect zone at 70°F. The 0.060-inch material exhibited the greatest growth in the weld centerline. It was difficult to establish which region of the 0.030-inch stock exhibited the greatest growth, although it appeared to be the weld centerline.

Based on the slow growth observations, it is important that static fracture toughness data be obtained so that failures occur in the stress range corresponding to the anticipated proof stress. For the Apollo hardware, this implies 70°F static toughness tests in the 140 ksi range and -320°F tests in the 187 ksi range. For the flaw sizes that will cause failures at these stresses, slow flaw growth is not significant.

The data generated in this program confirms the great value of the cryogenic proof tests for establishing the highest possible reliability in hardware. It is also apparent that a room temperature proof test prior to cryogenic proof testing is still a satisfactory technique to screen out the larger flaws. Performance of a room temperature proof test is less expensive than a cryogenic proof and if flaws are sufficiently large to cause failure in a room temperature proof, the screening operation is greatly simplified. There is also the possibility, although not great, that the room temperature proof test may result in leakage rather than catastrophic failure. If leakage occurs, the vessels could possibly be salvaged by suitable repair processes. The cryogenic proof test will screen out smaller flaws and will permit only vessels of high reliability to enter service.

IX. REFERENCES

1. C. F. Tiffany and J. N. Masters: *Investigation of the Flaw Growth Characteristics of 6Al-4V Titanium Used in Apollo Spacecraft Pressure Vessels.* NASA CR-65586, March 1967.

2. J. N. Masters: *Cyclic and Sustained Load Flaw Growth Characteristics of 6Al-4V Titanium.* NASA CR-92231, July 1968.

3. W. D. Bixler: *Comparison of Flaw Growth Characteristics under Cryogenic Proof and Ambient Test Conditions for Apollo Titanium Pressure Vessels.* NAS9-10265, The Boeing Company, January 1970.

4. David W. Hoeppner, Donald E. Pettit, Charles E. Feddersen, and Walter S. Hyler: *Determination of Flaw Growth Characteristics of Ti 6Al-4V Sheet in the Solution-Treated and Aged Condition.* NAS9-6969. Battelle Memorial Institute, January 1968.

5. F. R. Schwartzberg, *et al.: Interim Report - Cryogenic Alloy Screening.* NASA CR-72617, October 1969.

6. G. R. Irwin: "Crack-Extension Force for a Part-Through Crack in a Plate." *Journal of Applied Mechanics,* Vol 84E, No. 4, December 1962, pp 651 thru 654.

7. A. S. Kobayashi: *On the Magnification Factors of Deep Surface Flaws.* Structural Development Research Memorandum No. 16. The Boeing Company, December 1965.

8. F. W. Smith: *Stress-Intensity Factors for a Semielliptical Flaw.* Structural Development Research Memorandum No. 17. The Boeing Company, August 1966.

9. L. J. Larson: *Depth Effect for Semielliptical Surface Flaws.* R-69-14. Martin Marietta Corporation, Denver, Colorado, October 1969.

10. F. W. Smith: *Stress-Intensity Factors for Surface-Flawed Fracture Specimens.* R-69-15. Martin Marietta Corporation, Denver, Colorado, October 1969.

11. C. F. Tiffany, P. M. Lorenz, and L. R. Hall: *Investigation of Plane-Strain Flaw Growth in Thick-Walled Tanks.* NASA CR-54837. The Boeing Company, February 1966.

12. L. R. Hall: *Plane-Strain Cyclic Flaw Growth in 2014-T62 Aluminum and 6Al-4V (ELI) Titanium.* NASA CR-72396. The Boeing Company, November 1968.

APPENDIX

TABULATED EXPERIMENTAL DATA

Table A-1 Tensile Properties of Stress Relieved 6Aℓ-4V STA Titanium at Room Temperature (70°F)

LOCATION*	ULTIMATE TENSILE STRENGTH (ksi)	YIELD STRENGTH 0.2% OFFSET (ksi)	ELONGATION (% in 2 in.)
0.090-INCH THICKNESS			
Parent Metal	166.4	158.4	10.0
	164.8	158.2	10.0
	166.7	156.9	10.0
	(166.0 avg)	(158.0 avg)	(10.0 avg)
Heat Affected Zone	148.4	142.3	2.0
	148.7	142.1	2.5
	150.8	134.2	2.5
	(149.3 avg)	(139.5 avg)	(2.3 avg)
Weld Centerline	148.1	132.2	2.5
	147.1	129.6	2.5
	149.8	132.1	2.5
	(148.0 avg)	(131.3 avg)	(2.5 avg)
0.060-INCH THICKNESS			
Parent Metal	168.0	159.5	8.5
	169.8	159.2	7.5
	169.3	159.3	9.0
	(168.5 avg)	(159.3 avg)	(8.3 avg)
Heat Affected Zone	153.1	147.8	2.5
	152.9	135.8	2.5
	156.9	146.9	2.5
	(154.3 avg)	(147.3 avg)	(2.5 avg)
Weld Centerline	153.9	130.0	2.5
	154.2	133.6	2.5
	155.6	127.7	3.0
	(154.9 avg)	(130.1 avg)	(2.7 avg)
0.030-INCH THICKNESS			
Parent Metal	155.4	144.6	9.0
	166.8	155.8	8.0
	162.5	150.7	8.5
	(161.6 avg)	(150.4 avg)	(8.5 avg)
Heat Affected Zone	150.4	145.4	- †
	146.9	144.8	1.5
	155.6	139.2	2.0
	(151.0 avg)	(143.1 avg)	(1.8 avg)
Weld Centerline	149.3	126.4	1.5
	152.5	129.1	1.5
	(151.9 avg)	(127.7 avg)	(1.5 avg)

*For welded specimens, location denotes region where strain gage was placed for yield strength determination.

†Failed outside gage length.

Table A-2 Tensile Properties of Stress Relieved 6Aℓ-4V STA Titanium at Liquid Nitrogen Temperature (-320°F)

LOCATION*	ULTIMATE TENSILE STRENGTH (ksi)	YIELD STRENGTH, 0.2% OFFSET (ksi)
0.090 INCH THICKNESS		
Parent Metal	256.4	245.9
	254.0	244.8
	255.9	- †
	(255.4 avg)	(245.4 avg)
Heat Affected Zone	266.3	-
	235.6	221.2
	233.0	224.8
	(231.4 avg)	(223.0 avg)
Weld Centerline	232.3	218.1
	229.9	205.3
	237.1	219.2
	(229.8 avg)	(214.2 avg)
0.060-INCH THICKNESS		
Parent Metal	255.7	245.8
	256.8	244.2
	254.8	247.4
	(255.7 avg)	(245.7 avg)
Heat Affected Zone	243.9	224.6
	245.2	233.5
	241.7	- †
	(243.6 avg)	(229.1 avg)
Weld Centerline	244.6	218.1
	253.7	235.8
	239.6	216.8
	(246.0 avg)	(217.5 avg)
0.030-INCH THICKNESS		
Parent Metal	245.9	231.9
	252.6	242.3
	248.0	- †
	(248.8 avg)	(237.1 avg)
Heat Affected Zone	254.3	231.6
	253.9	237.5
	(254.1 avg)	(234.6 avg)
Weld Centerline	252.4	243.1
	253.2	247.9
	(252.8 avg)	(245.5 avg)

*For welded specimens, location denotes region where strain gage was placed for yield strength determination.

†Strain gage slipped or failed.

Table A-3 Static Fracture Toughness of 0.090-inch 6Al-4V STA Titanium at Room Temperature (70°F)

SPECIMEN NO.	FLAW SIZE			FRACTURE LOAD (lb)	FRACTURE STRESS (ksi)	FRACTURE/ YIELD STRESS RATIO	FRACTURE TOUGHNESS, K_{Ic} (ksi $\sqrt{in.}$)	REMARKS
	DEPTH, a (in.)	LENGTH, 2c (in.)	SHAPE a/Q					
PARENT METAL								
9CP-9	0.0447	0.2157	0.0382	27,300	139.1	0.88	52.6	
9CP-10	0.0577	0.3169	0.0489	23,300	117.8	0.74	50.8	
9CP-11	0.0554	0.2890	0.0465	22,100	112.9	0.71	47.6	
9CP-13	0.0538	0.1447	0.0313	28,750	147.4	0.92	50.9	
9CP-14	0.0540	0.2682	0.0454	24,400	123.4	0.78	51.2	
9CP-16	0.0620	0.1480	0.0330	28,050	141.4	0.89	50.2	
9CP-18	0.0634	0.1705	0.0360	27,500	141.4	0.89	52.4	Proof test failure
9CP-19	0.0603	0.1525	0.0328	28,750	144.8	0.92	51.1	Proof test failure
							(50.8 avg)	
WELD CENTERLINE								
9W3-1	0.0481	0.2293	0.0422	27,500	135.6	1.03	53.4	
9W3-4	0.0650	0.1542	0.0348	28,500	140.3	1.07	50.9	
9W6-3	0.0806	0.1914	0.0426	27,000	133.1	1.01	53.5	
9W2-2	0.0792	0.1952	0.0435	27,100	135.5	1.03	55.0	
9W9-5	0.0746	0.2057	0.0454	25,800	130.1	0.99	54.0	Proof test failure
							(53.4 avg)	
HEAT AFFECTED ZONE								
9W4-2	0.0422	0.2036	0.0367	26,600	131.9	0.94	50.2	
9W4-4	0.0790	0.1794	0.0393	25,700	125.9	0.90	48.6	
9W4-6	0.0718	0.1630	0.0355	25,800	133.9	0.91	49.0	
9W12-3	0.0658	0.1757	0.0387	27,150	135.5	0.97	52.1	Proof test failure
9W7-6	0.0438	0.2590	0.0409	27,000	131.5	0.94	51.8	Proof test failure
9W8-1	0.0425	0.2535	0.0405	26,500	133.2	0.96	52.2	Proof test failure
							(50.6 avg)	

Table A-4 Static Fracture Toughness of 0.060-inch 6Aℓ-4V STA Titanium at Room Temperature (70°F)

SPECIMEN NO.	FLAW SIZE			FRACTURE LOAD (lb)	FRACTURE STRESS (ksi)	FRACTURE YIELD STRESS RATIO	FRACTURE TOUGHNESS K_{Ic} (ksi$\sqrt{in.}$)	REMARKS
	DEPTH, a (in.)	LENGTH, 2c (in.)	SHAPE a/Q					
PARENT METAL								
6CP-13	0.0465	0.1003	0.0226	22,000	158.0	0.98	46.2	
6CP-14	0.0312	0.1162	0.0240	21,500	154.8	0.96	46.8	
6CP-2	0.0516	0.1470	0.0311	18,700	137.5	0.86	47.2	Proof Test Failure
6CP-5	0.0252	0.1559	0.0245	21,100	154.5	0.95	47.0	
6CP-21	0.0336	0.2325	0.0326	19,400	140.9	0.88	49.5	Proof Test Failure
6CP-20	0.0340	0.2527	0.0337	19,500	140.8	0.87	50.5	Proof Test Failure
13	0.0295	0.1471	0.0252	13,900	139.8	0.86	43.3	
							(47.2 avg)	
WELD CENTERLINE								
6W3-1	0.0618	0.1484	0.0337	19,450	134.8	1.04	48.4	
6W3-2	0.0562	0.1534	0.0329	19,600	138.6	1.07	48.9	
6W4-4	0.0307	0.1710	0.0298	21,000	141.5	1.09	47.5	
6W9-2	0.0534	0.1558	0.0345	15,500	133.0	1.02	48.2	Proof Test Failure
							(48.2 avg)	
HEAT AFFECTED ZONE								
6W4-2	0.0420	0.1350	0.0290	21,000	144.0	0.98	47.7	
6W4-3	0.0506	0.1287	0.0299	20,900	141.5	0.96	47.5	
6W3-3	0.0439	0.3170	0.0422	17,600	119.2	0.81	47.7	
6W5-10	0.0334	0.2188	0.0324	17,000	135.8	0.92	47.7	Proof Test Failure
							(47.6 avg)	

Table A-5 Static Fracture Toughness of 0.030-inch 6Aℓ-4V STA Titanium at Room Temperature (70°F)

SPECIMEN NO.	FLAW SIZE			FRACTURE LOAD (lb)	FRACTURE STRESS (ksi)	FRACTURE/ YIELD STRESS RATIO	FRACTURE TOUGHNESS K_{Ic} (ksi$\sqrt{in.}$)	REMARKS
	DEPTH, a (in.)	LENGTH, 2c (in.)	SHAPE a/Q					
PARENT METAL								
3CP-5	0.0160	0.1507	0.0178	9850	147.2	0.98	38.5	
3CP-7	0.0190	0.1696	0.0202	9600	143.1	0.95	39.6	
3CP-6	0.0185	0.1672	0.0201	9800	146.5	0.97	40.6	
3CP-12	0.0188	0.2169	0.0211	9400	140.5	0.93	39.7	Proof test failure
							(39.6 avg)	
WELD CENTERLINE								
3W2-6	0.0154	0.1620	0.0179	9000	133.9	1.05	35.0	
3W2-3	0.0183	0.1715	0.0203	8750	127.2	1.00	35.2	
3W3-1	0.0179	0.1700	0.0203	8800	126.8	0.99	35.1	Proof test failure
3W4-1	0.0166	0.1540	0.0184	9000	129.5	1.01	(34.3)	Proof test failure
							(34.9 avg)	
HEAT AFFECTED ZONE								
3W3-3	0.0194	0.1805	0.0202	8500	123.7	0.86	34.3	
3W2-4	0.0156	0.1612	0.0173	9200	134.7	0.94	34.7	
3W2-7	0.0151	0.1663	0.0162	8600	121.8	0.85	(30.2)	Proof test failure
							(33.1 avg)	

Table A-6 Static Fracture Toughness of 0.090-inch 6Al-4V STA Titanium at -320°F

SPECIMEN NO.	FLAW SIZE			FRACTURE LOAD (lb)	FRACTURE STRESS (ksi)	FRACTURE/ YIELD STRESS RATIO	FRACTURE TOUGHNESS, K_{Ic} (ksi$\sqrt{in.}$)	REMARKS
	DEPTH, a (in.)	LENGTH, 2c (in.)	SHAPE a/Q					
PARENT METAL								
9CP-22	0.0465	0.1284	0.0261	28,750	143.5	0.58	45.3	
9CP-24	0.0305	0.0830	0.0176	42,500	210.9	0.86	54.7	
9CP-35	0.0433	0.2244	0.0346	24,250	119.4	0.49	43.3	
9CP-29	0.0383	0.2384	0.0327	28,500	142.5	0.58	50.3	
9CP-33	0.0374	0.2254	0.0322	30,100	149.2	0.61	52.4	
9CP-25	0.0310	0.0868	0.0180	38,500	192.1	0.78	50.2	
9CP-28	0.0415	0.2355	0.0349	23,200	116.6	0.48	42.5	
9CP-32	0.0453	0.2519	0.0374	26,500	131.3	0.54	49.4	
9CP-34	0.0395	0.1014	0.0214	37,000	184.0	0.75	52.4	
9DP-3	0.0215	0.0852	0.0164	36,000	207.9	0.85	51.9	Proof test failure
9DP-4	0.0285	0.1027	0.0194	28,200	162.5	0.66	44.1	Proof test failure
							(48.7 avg)	
WELD CENTERLINE								
9W5-6	0.0328	0.0826	0.0185	44,000	222.9	1.04	59.1	
9W3-6	0.0454	0.1052	0.0230	39,250	193.0	0.90	57.2	
9W6-2	0.0368	0.2236	0.0340	38,250	187.7	0.88	67.3	
9W7-4	0.0425	0.2465	0.0383	35,750	176.3	0.82	67.4	
9W8-6	0.0420	0.2500	0.0375	32,700	164.5	0.77	62.2	
9W4-5	0.0561	0.1531	0.0328	37,500	184.9	0.86	65.3	
9W6-1	0.0370	0.1062	0.0226	38,500	191.1	0.89	55.9	
9W8-5	0.0445	0.2458	0.0377	28,750	144.9	0.68	54.8	
9W7-3	0.0465	0.2510	0.0394	29,500	147.7	0.69	57.3	
9W15-1	0.0370	0.1230	0.0245	26,400	162.6	0.76	49.8	Proof test failure
							(59.6 avg)	
HEAT AFFECTED ZONE								
9W5-2	0.0540	0.1396	0.0293	35,000	172.7	0.77	57.6	
9W9-6	0.0360	0.1060	0.0212	39,750	199.3	0.89	56.7	
9W10-1	0.0414	0.2250	0.0351	28,750	147.0	0.66	53.8	
9W8-2	0.0360	0.2270	0.0321	31,000	153.9	0.69	53.7	
9W9-4	0.0404	0.2326	0.0345	29,250	144.0	0.65	52.2	
9W6-4	0.0354	0.0983	0.0211	40,750	205.1	0.92	58.0	
9W9-3	0.0440	0.2536	0.0376	29,000	145.6	0.65	55.0	
9W6-6	0.0689	0.1835	0.0381	28,750	143.0	0.64	54.4	
							(55.1 avg)	

Table A-7 Static Fracture Toughness of 0.060-inch 6Aℓ-4V STA Titanium at -320°F

SPECIMEN NO.	FLAW SIZE			FRACTURE LOAD (lb)	FRACTURE STRESS (ksi)	FRACTURE/ YIELD STRESS RATIO	FRACTURE TOUGHNESS, K_{Ic} (ksi $\sqrt{in.}$)	REMARKS
	DEPTH, a (in.)	LENGTH, 2c (in.)	SHAPE a/Q					
PARENT METAL								
6CP-16	0.0276	0.0722	0.0155	28,500	206.0	0.84	50.2	
6CP-10	0.0348	0.0827	0.0176	25,000	183.6	0.75	47.3	
6DP-16	0.0231	0.1200	0.0193	26,200	186.9	0.76	50.7	Proof test
6CP-23	0.0282	0.2330	0.0254	14,150	101.9	0.41	31.7	
6CP-7	0.0307	0.1868	0.0262	18,500	135.9	0.55	42.9	
6CP-19	0.0274	0.0728	0.0157	25,500	182.5	0.74	44.5	
6CP-1	0.0368	0.1037	0.0210	20,500	152.9	0.62	43.2	
6CP-15	0.0335	0.2170	0.0291	17,850	129.0	0.52	43.0	
6CP-18	0.0252	0.0718	0.0150	27,800	200.1	0.81	48.0	
6CP-30	0.0207	0.0555	0.0122	>31,000	>227.6	>0.93	>49.3	Broke in grip; proof test
6DP-15	0.0305	0.1715	0.0248	18,200	133.9	0.54	41.0	
6DP-14	0.0266	0.0875	0.0186	33,500	238.1	0.97	63.1	Insufficient flaw growth of precrack
6DP-1	0.0190	0.0746	0.0147	>30,500	>230.5	0.94	>54.4	Broke in grip
							(46.0 avg)	
WELD CENTERLINE								
6W3-6	0.0279	0.0698	0.0153	34,000	229.1	0.94	55.4	
6W3-7	0.0359	0.1231	0.0241	27,300	177.7	0.73	53.7	
6W4-5	0.0248	0.0692	0.0148	29,500	232.6	1.00	56.4	
6W4-6	0.0342	0.2070	0.0300	21,300	168.1	0.69	56.7	
6W4-7	0.0322	0.2056	0.0275	15,300	119.3	0.49	38.6	
6W6-2	0.0305	0.1205	0.0223	19,700	158.5	0.65	46.4	Proof test failure
							(51.2 avg)	
HEAT AFFECTED ZONE								
6W3-10	0.0315	0.0834	0.0178	28,300	200.3	0.87	52.0	
6W4-8	0.0248	0.0665	0.0146	27,000	216.0	0.94	51.0	
6W4-9	0.0356	0.2164	0.0302	14,400	111.2	0.48	37.7	
6W4-10	0.0281	0.2070	0.0268	19,900	154.7	0.68	49.5	
							(47.5 avg)	

Table A-8 Static Fracture Toughness of 0.030-inch 6Al-4V STA Titanium at -320°F

SPECIMEN NO.	FLAW SIZE			FRACTURE LOAD (lb)	FRACTURE STRESS (psi)	FRACTURE/ YIELD STRESS Ratio	FRACTURE TOUGHNESS K_{Ic} $(ksi\sqrt{in.})$	REMARKS
	DEPTH, a (in.)	LENGTH, 2c (in.)	SHAPE a/Q					
PARENT METAL								
3CP-8	0.0188	0.2200	0.0186	10,600	158.4	0.67	42.0	
3CP-9	0.0255	0.2217	0.0236	8,950	134.4	0.57	44.4	
3CP-10	0.0125	0.1525	0.0132	12,600	188.3	0.79	42.2	
3CP-14	0.0166	0.1579	0.0164	11,100	164.4	0.69	41.0	
3CP-18	0.0170	0.1562	0.0166	10,350	154.7	0.65	38.9	
3CP-17	0.0171	0.1703	0.0169	9,920	149.8	0.63	38.0	
							(41.0 avg)	
WELD CENTERLINE								
3W2-1	0.0150	0.1456	0.0150	12,000	172.7	1.00	41.1	
3W2-2	0.0242	0.2220	0.0230	9,750	141.3	1.05	41.9	
3W4-9	0.0206	0.1590	0.0187	8,860	137.3	1.10	36.7	
3W4-10	0.0184	0.1597	0.0179	10,780	164.8	1.03	42.7	
3W5-2	0.0183	0.1578	0.0176	10,850	160.0	1.04	41.2	
							(40.7 avg)	
HEAT AFFECTED ZONE								
3W2-7	0.0255	0.2390	0.0238	7,450	114.1	0.48	34.3	
3W2-8	0.0155	0.1449	0.0153	10,850	165.6	0.70	40.4	
3W2-9	0.0207	0.1618	0.0192	9,350	137.8	0.58	37.4	
3W5-4	0.0139	0.1620	0.0134	10,460	158.7	0.67	35.9	
3W5-5	0.0212	0.1669	0.0196	9,010	137.8	0.58	37.6	
3W5-6	0.0133	0.1464	0.0133	10,400	159.3	0.67	35.7	
3W3-10	0.0161	0.1627	0.0156	9,320	143.2	0.60	34.9	
							(36.6 avg)	

Table A-9 Proof Test Data for 0.090-inch 6Al-4V Titanium Tested In Air

SPECIMEN NO.	FLAW SIZE				PROOF STRESS (ksi	STRESS INTENSITY, K_{Ii} (ksi$\sqrt{in.}$)		STRESS INTENSITY RATIO K_{Ii}/K_{Ic}		FLAW GROWTH INITIATION		PROOF GROWTH				COMMENTS*
	DEPTH, a (in.)	LENGTH, 2c (in.)	SHAPE a/2c	a/Q		DESIRED	ACTUAL	DESIRED	ACTUAL	$\%K_{Ic}$	METHOD	TYPE	GROWTH (in.) AT INDICATED ANGLE 0° (Δa)	90° ($\Delta 2c$)	Ψ	
Parent Metal																
9CP-18	0.0634	0.1705	0.372	0.0360	141.4	51.0	52.4	1.00	1.03	NI	--	U	0.001	0.003		Failed during proof
9CP-19	0.0603	0.1525	0.395	0.0328	144.8	51.0	51.1	1.00	1.00	NI	--	U	0.002	0.003		Failed during proof
9CP-8	0.0564	0.1422	0.397	0.0310	140.7	48.5	48.3	0.95	0.95	0.92	SG,CG	NU	0.002	0.004	0.004 @ 65°	
9CP-20	0.0580	0.1425	0.407	0.0308	140.3	45.9	47.9	0.90	0.94	0.94	SG	T	0.003	0.013	0.016 @ 64°	
9CP-15	0.0480	0.1157	0.415	0.0253	140.3	40.8	43.5	0.80	0.85	NI	--	U	0.001	0.002		
9CP-26	0.0480	0.2395	0.200	0.0403	128.6	51.0	50.4	1.00	0.99	NI	--	NV				
9CP-27	0.0362	0.2298	0.158	0.0329	140.7	48.5	51.0	0.95	1.00	0.91	SG	NU	0.002			
Weld Centerline																
9W3-2	0.0755	0.2180	0.346	0.0468	124.1	53.4	52.3	1.00	0.98	0.87	SG,CG					Cracked through to backface during proof
9W9-5	0.0746	0.2057	0.363	0.0454	130.1	53.4	49.8	1.00	0.93	NI	--	NU	0.004	0.003	0.007 @ 30°	
9W5-1	0.0650	0.1860	0.349	0.0404	128.0	50.7	50.2	0.95	0.94	0.88	SG,CG	U	0.004	0.005		
9W2-1	0.0612	0.1702	0.360	0.0373	131.5	48.1	49.5	0.90	0.93	0.86	SG,CG	U	0.002	0.004		
9W7-1	0.0494	0.2655	0.186	0.0453	126.1	53.4	52.4	1.00	0.98	NI	--	U	0.003	0.008		
9W7-2	0.0430	0.2535	0.170	0.0413	130.8	50.7	51.8	0.95	0.97	0.91	SG	NV				
9W10-3	0.0428	0.2475	0.173	0.0382	121.9	50.7	46.2	0.95	0.87	NI	--	NU	0.0005	0.003	0.009 @ 80°	
Heat Affected Zone																
9W12-3	0.0658	0.1757	0.375	0.0387	135.5	50.6	52.1	1.00	1.03	NI	--	U	0.002	0.004		Failed during proof
9W12-6	0.0628	0.1586	0.396	0.0387	130.8	48.1	47.4	0.95	0.94	0.91	SG,CG	NU	0.006	0.014	0.009 @ 68°	
9W4-1	0.0508	0.1352	0.376	0.0294	128.4	45.5	42.8	0.90	0.85	NI	SG	U	0.0005	0.001		
9W3-5	0.0516	0.1221	0.423	0.0267	126.9	43.0	40.3	0.85	0.80	NI	SG	NV				
9W7-6	0.0438	0.2590	0.169	0.0409	131.5	50.6	51.8	1.00	1.02	0.96	SG,CG	U	0.0007	0.002		Failed during proof
9W8-1	0.0425	0.2535	0.168	0.0405	132.2	50.6	52.2	1.00	1.03	0.95	SG,CG	NU			0.003 @ 82°	Failed during proof
9W7-5	0.0456	0.2592	0.176	0.0396	130.3	50.6	50.6	1.00	1.00	NI	--	NV				
9W10-2	0.0417	0.1751	0.236	0.0382	127.6	48.1	48.5	0.95	0.96	0.91	SG	NU	0.002	0.001	0.008 @ 75°	

CODE:

NI - no indication; NU - nonuniform;
SG - strain gage; T - tunneling;
CG - compliance gage; NV - no visible growth indication.
U - uniform flaw growth;

*All hold times 15 seconds.

Table A-10 Proof Test Data for 0.090-inch 6Al-4V Titanium Tested in Water

SPECIMEN NO.	FLAW SIZE				PROOF STRESS (ksi)	STRESS INTENSITY, K_{Ii} (ksi $\sqrt{in.}$)		STRESS INTENSITY RATIO K_{Ii}/K_{Ic}		FLAW GROWTH INITIATION		PROOF GROWTH				COMMENTS*
	DEPTH, a (in.)	LENGTH, 2c (in.)	SHAPE a/2c	a/Q		DESIRED	ACTUAL	DESIRED	ACTUAL	$\%K_{Ic}$	METHOD	TYPE	GROWTH (in.) AT INDICATED ANGLE: 0° (Δa)	90° (Δ2c)	ψ	
Parent Metal																
9CP-7	0.0656	0.1668	0.393	0.0363	140.4	51.0	52.2	1.00	1.02	NI	--	T	0.004	0.069	0.040 @ 70°	
9CP-12	0.0553	0.1631	0.339	0.0345	142.2	48.5	51.6	0.95	1.01	0.95	SG	T	0.005	0.045	0.031 @ 70°	
9CP-21	0.0476	0.1300	0.366	0.0278	137.2	45.9	44.7	0.90	0.88	NI	--	U	0.002	0.003		
9CP-30	0.0442	0.2356	0.188	0.0384	127.7	51.0	48.8	1.00	0.96	0.90	CG	U	0.004	0.006		
9CP-31	0.0438	0.2374	0.184	0.0388	132.1	48.5	50.7	0.95	0.99	0.94	CG	U	0.003	0.005		
Weld Centerline																
9W2-3	0.0495	0.1930	0.256	0.0386	128.3	53.4	49.0	1.00	0.92	NI	--	NU	0.004	0.002	0.010 @ 58°	
9W2-4	0.0619	0.1737	0.356	0.0380	131.3	50.7	49.9	0.95	0.93	0.87	SG	U	0.005	0.013		
9W3-3	0.0600	0.1696	0.354	0.0370	130.4	48.1	48.8	0.90	0.91	NI	--	U	0.003	0.008		
9W8-3	0.0452	0.2447	0.185	0.0418	127.0	53.4	50.5	1.00	0.95	NI	--	NU	0.001	0.009	0.013 @ 81°	
9W8-4	0.0357	0.2264	0.158	0.0355	129.5	50.7	48.0	0.95	0.90	0.87	SG	NU	0.008	0.007	0.011 @ 82°	
Heat Affected Zone																
9W4-3	0.0720	0.1874	0.0384	0.0409	132.5	50.6	52.2	1.00	1.03	0.92	SG,CG	NV				Failed during proof
9W6-5	0.0620	0.1655	0.375	0.0363	129.5	48.1	48.2	0.95	0.95	0.90	SG	U	0.003	0.006		
9W5-4	0.0560	0.1431	0.391	0.0313	127.4	45.5	44.0	0.90	0.87	0.78	SG	NU	0.0006	0.001	0.004 @ 70°	
9W9-1	0.0426	0.2459	0.173	0.0398	131.0	50.6	50.8	1.00	1.00	NI	--	U	0.001	0.003		
9W9-2	0.0423	0.2506	0.169	0.0399	128.6	48.1	49.9	0.95	0.99	0.94	SG	NU	0.005	0.003	0.006 @ 66°	

CODE:

NI - no indication; NU - nonuniform;
SG - strain gage; T - tunneling;
CG - compliance gage; NV - no visible growth indication.
U - uniform flaw growth;

*All hold times 15 seconds.

Table A-11 Proof Test Data for 0.090-inch 6Al-4V Titanium Tested in Liquid Nitrogen

SPECIMEN NO.	FLAW SIZE				PROOF STRESS (ksi)	STRESS INTENSITY, K_{Ii} (ksi$\sqrt{in.}$)		STRESS INTENSITY RATIO (K_{Ii}/K_{Ic})		FLAW GROWTH INITIATION		PROOF GROWTH				FRACTURE FACE VISUAL OBSERVATIONS	COMMENTS*
	DEPTH, a (in.)	LENGTH, 2c (in.)	SHAPE a/2c	a/Q		DESIRED	ACTUAL	DESIRED	ACTUAL	$\%K_{Ic}$	METHOD	TYPE	GROWTH (in.) AT INDICATED ANGLE 0° (Δa)	90° (2c)	Ψ		
Parent Metal																	
9DP-7	0.0397	0.1146	0.346	0.0232	150.7	48.7	44.7	1.00	0.92	NI	--	NU			0.001 @ 75°	NU	Failed during proof
9DP-9	0.0332	0.0884	0.376	0.0185	188.4	46.3	50.0	0.95	1.03	NI	--	U	0.002	0.003		U	
9CP-45	0.0300	0.0916	0.327	0.0185	175.5	41.4	46.5	0.85	0.95	NI	--	NU	0.002	0.002	0.002 @ 63°	NU	
9DP-3	0.0207	0.0805	0.244	0.0164	212.4	48.7	51.9	1.00	1.06	NI	--	NU			0.006 @ 68°	NU	Failed during proof
9DP-4	0.0289	0.1014	0.285	0.0191	164.9	46.3	44.3	0.95	0.91	NI	--	NU			0.001 @ 28°	NU	Failed during proof
9CP-47	0.268	0.0832	0.322	0.0168	184.4	41.4	46.7	0.85	0.96	NI	--	NV				NV	
Weld Centerline																	
9W11-4	0.0368	0.0992	0.371	0.0213	214.2	59.6	52.2	1.00	0.88	0.82	SG, CG	NU			0.024 @ 66°	NU	Failed during proof
9W15-1	0.0370	0.1230	0.301	0.0245	162.6	59.6	49.8	1.00	0.84	NI	--	U	0.001	0.002		U	Failed during proof
9W11-2	0.0324	0.0902	0.359	0.0191	183.6	56.6	49.4	0.95	0.83	NI	--	NV				NV	
9W10-6	0.0345	0.1096	0.314	0.0212	185.4	59.6	52.8	1.00	0.89	NI	--	NV				NV	
9W10-4	0.0305	0.0931	0.328	0.0193	185.7	56.6	50.3	0.95	0.84	NI	--	NV				NV	
9W15-2	0.0255	0.0872	0.292	0.0177	185.3	50.7	48.1	0.85	0.81	NI	--	NV				NV	
Heat Affected Zone																	
9W11-5	0.0395	0.1298	0.304	0.0263	185.9	55.1	58.7	1.00	1.06	NI	--	NU	0.002	0.004	0.003 @ 68°	NU	
9W11-3	0.0370	0.1158	0.319	0.0255	185.5	52.3	57.9	0.95	1.05	NI	--	NV				NV	
9W15-3	0.0310	0.1028	0.301	0.0210	188.3	55.1	53.2	1.00	0.96	NI	--	NU	0.002	0.004	0.008 @ 56°	NU	
9W11-1	0.0320	0.1130	0.283	0.0225	192.0	55.1	54.7	1.00	0.99	NI	--	NV				NV	
9W10-5	0.0223	0.0850	0.262	0.0164	186.8	49.6	46.6	0.90	0.85	NI	--	NV				NV	
9W15-6	0.0228	0.0904	0.252	0.0171	183.3	46.8	46.8	0.85	0.85	NI	--	NV				NV	

CODE:

NI - no indication; NU - nonuniform;
SG - strain gage; T - tunneling;
CG - compliance gage; NV - no visible growth indication.
U - uniform flaw growth;

*All hold times 15 seconds.

Table A-12 Proof Test Data for 0.060-inch 6Al-4V Titanium Tested in Air

SPECIMEN NO.	FLAW SIZE				PROOF STRESS (ksi)	STRESS INTENSITY, K_{Ii} (ksi$\sqrt{in.}$)		STRESS INTENSITY RATIO (K_{Ii}/K_{Ic})		FLAW GROWTH INITIATION		PROOF GROWTH				COMMENTS*
	DEPTH, a (in.)	LENGTH, 2c (in.)	SHAPE a/2c	a/Q		DESIRED	ACTUAL	DESIRED	ACTUAL	%K_{Ic}	METHOD	TYPE	GROWTH (in.) AT INDICATED ANGLE 0° (Δa)	90° (2c)	ψ	
Parent Metal																
6CP-2	0.0516	0.1470	0.351	0.0311	137.5	47.2	47.2	1.00	1.00	NI	--	T			0.022 @ 72°	
6CP-3	0.0446	0.1287	0.346	0.0271	141.7	44.8	45.6	0.95	0.97	0.91	SG	U	0.002	0.003		
6CP-4	0.0422	0.1049	0.403	0.0228	141.5	42.5	41.7	0.90	0.88	NI	--	U	0.003	0.006		
6CP-6	0.0354	0.2133	0.166	0.0311	143.2	47.2	50.8	1.00	1.08	0.95	CG	NU (Some tunneling on one side of flaw)	0.002	0.008	0.011 @ 77°	
6CP-11	0.0276	0.2137	0.129	0.0279	142.2	44.8	46.3	0.95	0.98	0.93	SG, CG	NU	0.003			
6DP-18	0.0469	0.1361	0.345	0.0288	138.2	47.2	45.8	1.00	0.97	NI	--	U	0.005	0.009		30 minute hold
6CP-26	0.0485	0.1309	0.371	0.0280	135.4	44.8	44.1	0.95	0.93	0.88	CG	U	0.001	0.004		30 minute hold
6DP-3	0.0360	0.2222	0.162	0.0336	139.8	47.2	49.9	1.00	1.06	0.95	CG	U	0.006	0.010		30 minute hold
6CP-27	0.0283	0.2078	0.136	0.0277	137.9	44.8	44.6	0.95	0.94	NI	--	NU	0.001	0.001	0.002 @ 74°	30 minute hold
Weld Centerline																
6W9-10	0.0438	0.1444	0.303	0.0313	135.6	48.2	46.8	1.00	0.97	NI	--	U	0.002	0.004		Failed during proof
6W3-8	0.0456	0.1335	0.342	0.0292	136.2	45.8	45.4	0.95	0.94	0.89	SG, CG	NU	0.007	0.006	0.010 @ 68°	
6W5-1	0.0340	0.1975	0.121	0.0378	140.2	48.2	53.0	1.00	1.10	NI	--	U	0.003	0.007		Failed during proof
6W5-2	0.0356	0.2196	0.162	0.0352	134.1	45.8	49.2	0.95	1.02	0.98	SG, CG	NU	0.006			
Heat Affected Zone																
6W4-3	0.0473	0.1395	0.339	0.0299	140.7	47.6	47.5	1.00	1.00	0.94	SG	U	0.002	0.004		Failed during proof
6W3-4	0.0506	0.1287	0.393	0.0283	141.5	45.2	46.4	0.95	0.97	0.91	SG	U	0.003	0.006		
6W5-8	0.0293	0.2142	0.137	0.0293	135.6	45.2	45.2	0.95	0.95	0.91	SG, CG	NU	0.003	0.0005		
6W5-5	0.0317	0.2002	0.158	0.0308	138.7	45.2	47.3	0.95	0.99	NI	--	NU	0.003	0.003		

CODE:

NI - no indication;
SG - strain gage;
CG - compliance gage;
U - uniform flaw growth;
NU - nonuniform
T - tunneling;
NV - no visible growth indication.

*All hold times 15 seconds, except where noted.

Table A-13 Proof Test Data for 0.060-Inch 6Al-4V Titanium Tested in Water

SPECIMEN NO.	FLAW SIZE				PROOF STRESS (ksi)	STRESS INTENSITY, K_{Ii} (ksi$\sqrt{in.}$)		STRESS INTENSITY RATIO (K_{Ii}/K_{Ic})		FLAW GROWTH INITIATION		PROOF GROWTH				* COMMENTS
	DEPTH, a (in.)	LENGTH, 2c (in.)	SHAPE a/2c	a/Q		DESIRED	ACTUAL	DESIRED	ACTUAL	$\%K_{Ic}$	METHOD	TYPE	GROWTH (in.) AT INDICATED ANGLE 0° (Δa)	90° ($\Delta 2c$)	Ψ	
Parent Metal																
6CP-9	0.0510	0.1390	0.367	0.0295	132.6	47.2	44.5	1.00	0.94	0.89	SG	NU	0.001	0.004	0.006 @ 73°	
6CP-17	0.0461	0.1314	0.351	0.0279	141.0	44.8	45.9	0.95	0.98	NI	--	NU	0.001	0.003	0.006 @ 72°	
6CP-20	0.0340	0.2527	0.134	0.0337	140.8	47.2	50.5	1.00	1.07	NI	--	T			0.037 @ 81°	Failed during proof
6CP-21	0.0336	0.2325	0.145	0.0326	140.9	47.2	49.5	1.00	1.05	NI	--	T			0.044 @ 79°	Failed during proof
6DP-13	0.0362	0.2130	0.170	0.0332	139.6	44.8	49.8	0.95	1.05	NI	--	NU	0.002	0.003	0.011 @ 78°	
6CP-22	0.0344	0.2049	0.168	0.0319	140.4	44.8	49.0	0.95	1.04	0.98	SG	NU	0.003	0.003		
6DP-4	0.0491	0.1347	0.365	0.0288	142.3	47.2	47.2	1.00	1.00	0.90	SG, CG	T			0.030 @ 75°	30 minute hold
6CP-28	0.0463	0.1318	0.351	0.0279	139.5	44.8	45.4	0.95	0.96	0.89	SG	NU	0.002	0.005	0.003 @ 70°	30 minute hold
6DP-5	0.0354	0.2153	0.164	0.0327	138.9	47.2	49.0	1.00	1.04	NI	--	NU	0.005	0.009		30 minute hold
6CP-29	0.0264	0.2083	0.127	0.0272	140.2	44.8	45.1	0.95	0.96	NI	--	NU	0.003	0.0007		30 minute hold
Weld Centerline																
6W9-2	0.0534	0.1558	0.343	0.0345	133.0	48.2	48.2	1.00	1.00	NI	--	NV				Failed during proof
6W3-9	0.0583	0.1614	0.361	0.0355	129.7	45.8	47.5	0.95	0.98	0.92	SG	NU	0.003	0.002	0.009 @ 44°	
6W5-3	0.0365	0.2115	0.173	0.0351	133.2	48.2	48.6	1.00	1.01	NI	--	U	0.002	0.004		Failed during proof
6W5-4	0.0340	0.2159	0.157	0.0340	136.1	45.8	48.8	0.95	1.01	0.94	SG	NU			0.005 @ 60°	
Heat Affected Zone																
6W9-3	0.0512	0.1468	0.349	0.0330	130.0	47.6	46.1	1.00	0.97	0.83	SG	NU			0.006 @ 78°	Failed during proof
6W3-5	0.0480	0.1330	0.361	0.0286	135.2	45.2	44.6	0.95	0.94	0.88	SG	NU	0.0005	0.004	0.004 @ 84°	
6W5-10	0.0334	0.2188	0.153	0.0324	135.8	47.6	47.7	1.00	1.00	0.86	SG	NV				Failed during proof
6W5-9	0.0347	0.2165	0.160	0.0330	135.3	45.2	48.0	0.95	1.01	NI	--	NU	0.003	0.002		
6W9-7	0.0302	0.2004	0.151	0.0299	138.6	45.2	46.8	0.95	0.98	NI	--	NU	0.001	0.003	0.004 @ 85°	Failed during proof

*All hold times 15 seconds.

CODE:

NI - no indication; NU - nonuniform
SG - strain gage; T - tunneling;
CG - compliance gage; NV - no visible growth indication.
U - uniform flaw growth;

Table A-14 Proof Test Data for 0.060-inch 6Al-4V Titanium Tested in Liquid Nitrogen

SPECIMEN NO.	FLAW SIZE				PROOF STRESS (ksi)	STRESS INTENSITY, K_{Ii} (ksi$\sqrt{in.}$)		STRESS INTENSITY RATIO (K_{Ii}/K_{Ic})		FLAW GROWTH INITIATION		PROOF GROWTH				COMMENTS*
	DEPTH, a (in.)	LENGTH, 2c (in.)	SHAPE a/2c	a/Q		DESIRED	ACTUAL	DESIRED	ACTUAL	$\%K_{Ic}$	METHOD	TYPE	GROWTH (in.) AT INDICATED ANGLE 0° (Δa)	90° (Δ2c)	∀	
Parent Metal																
6DP-11	0.290	0.0862	0.336	0.0176	189.3	43.7	49.1	0.95	1.07	NI	--	U	0.001	0.003		
6CP-30	0.208	0.0568	0.366	0.0122	212.9	46.0	45.7	1.00	0.99	NI	--	NU	0.002	0.003	0.002 @ 64°	Failed during proof
6DP-1	0.0190	0.0746	0.255	0.0147	230.5	46.0	54.4	1.00	1.18	NI	--	NU			0.004 @ 73°	Failed in grips during proof
6DP-14	0.0266	0.0875	0.304	0.0186	238.1	46.0	--	1.00	--	NI	--	NV				Failed during proof, no starter flaw groth
6DP-15	0.0305	0.1715	0.178	0.0248	133.9	46.0	41.0	1.00	0.89	NI	--	U	0.001	0.004		Failed during proof
6DP-16	0.0235	0.1192	0.197	0.0201	186.4	46.0	49.9	1.00	1.08	NI	--	NU	0.001	0.004	0.005 @ 74°	Failed during proof
6DP-12	0.0218	0.0909	0.240	0.0166	188.1	43.7	47.3	0.95	1.03	NI	--	U	0.002	0.003		
6CP-31	0.0230	0.0748	0.307	0.0153	203.8	46.0	49.3	1.00	1.07	NI	--	U	0.002	0.003		
6DP-7	0.0280	0.0864	0.324	0.0177	186.4	46.0	48.4	1.00	1.05	NI	--	U	0.001	0.002		30 minute hold; failed during proof
6DP-17	0.0255	0.0818	0.312	0.0165	184.2	43.7	46.0	0.95	1.05	NI	--	NU			0.001 @ 70°	Failed during proof
6DP-6	0.0268	0.0794	0.338	0.0162	187.9	46.0	46.5	0.95	1.01	NI	--	NU, T	0.006	0.003	0.012 @ 68°	30 minute hold
6DP-8	0.0236	0.1143	0.206	0.0192	172.8	46.0	46.8	1.00	1.02	NI	--	NU (tunneling on one side)	0.006	0.012	0.012 @ 64°	30 minute hold; failed during proof
6DP-9	0.0239	0.0932	0.256	0.0176	183.6	46.0	47.6	0.95	1.03	NI	--	NU (tunneling on one side)	0.001	0.004	0.004 @ 78°	30 minute hold
Weld Centerline																
6W8-7	0.0340	0.1160	0.293	0.0197	173.3	51.2	47.3	1.00	0.92	NI	--	NU	0.001	0.002	0.003 @ 76°	Failed during proof
6W9-5	0.0324	0.0948	0.342	0.0196	181.4	48.6	49.5	0.95	0.97	NI	--	NU			0.022 @ 74°	Failed during proof
6W6-2	0.0317	0.1070	0.296	0.0223	158.5	51.2	46.4	1.00	0.91	NI	--	NU	0.0008	0.011	0.013 @ 80°	Failed during proof
6W7-5	0.0233	0.0877	0.266	0.0171	171.9	51.2	43.6	1.00	0.85	NI	--	NU	0.0005	0.006	0.011 @ 75°	Failed during proof
6W7-2	0.0202	0.0830	0.243	0.0154	188.3	48.6	45.5	0.95	0.89	NI	--	NU (tunneling on side of flaw)			0.022 @ 68°	Failed during proof
6W6-4	0.0256	0.0846	0.303	0.0168	185.6	43.5	47.0	0.85	0.92	NI	--	NU	0.005	0.003		
6W9-9	0.0268	0.0774	0.346	0.0160	174.8	48.6	42.9	0.95	0.84	NI	--	NV				
Heat Affected Zone																
6W9-1	0.0334	0.1154	0.289	0.0230	187.8	47.5	55.7	1.00	1.17	NI	--	NU	0.003	0.003	0.008 @ 70°	Failed during proof
6W9-6	0.0293	0.0916	0.320	0.0188	186.4	45.1	49.8	0.95	1.05	NI	--	NV				
6W6-7	0.0263	0.0868	0.303	0.0174	186.7	40.4	48.1	0.85	1.01	NI	--	NV				
6W8-6	0.0231	0.0870	0.266	0.0172	190.5	47.5	48.6	1.00	1.02	NI	--	U	0.002	0.006		
6W9-8	0.0274	0.1576	0.174	0.0242	168.0	47.5	51.1	1.00	1.08	NI	--	NU			0.004 @ 77°	Failed during proof
6W7-3	0.0176	0.0815	0.216	0.0144	188.7	45.1	44.2	0.95	0.93	NI	--	NV				
6W7-1	0.0201	0.0768	0.262	0.0148	184.6	40.4	43.9	0.85	0.92	NI	--	NV				

CODE:

NI - no indication; NU - nonuniform;
SG - strain gage; T - tunneling;
CG - compliance gage; NV - no visible growth indication.
U - uniform flaw growth;

*All hold times 15 seconds except where noted.

Table A-15 Proof Test Data for 0.030-inch 6Al-4V Titanium Tested in Air

SPECIMEN NO.	FLAW SIZE				PROOF STRESS (ksi)	STRESS INTENSITY K_{Ii} (ksi$\sqrt{in.}$)		STRESS INTENSITY RATIO (K_{Ii}/K_{Ic})		FLAW GROWTH INITIATION		PROOF GROWTH				COMMENTS*
	DEPTH, a (in.)	LENGTH, 2c (in.)	SHAPE a/2c	a/Q		DESIRED	ACTUAL	DESIRED	ACTUAL	%K_{Ic}	METHOD	TYPE	GROWTH (in.) AT INDICATED ANGLE 0° (Δa)	90° (Δ2c)	Ψ	
Parent Metal																
3CP-12	0.0188	0.2169	0.087	0.0211	140.5	39.6	39.7	1.00	1.00	0.85	SG	NU (Tunneling on one side)			0.013 @ 86°	Failed during proof
3CP-11	0.0202	0.1921	0.105	0.0220	142.0	37.6	41.0	0.95	1.03	NI	--	NU				Cracked through to back-face
3CP-13	0.0172	0.1729	0.099	0.0185	134.5	35.6	35.7	0.90	0.90	NI	--	NV				
Weld Centerline																
3W3-1	0.0179	0.1700	0.095	0.0203	126.8	34.9	35.1	1.00	1.01	0.94	SG, CG	NV				Failed during proof
3W2-10	0.0201	0.1880	0.107	0.0228	138.2	34.9	40.7	1.00	1.17	NI	--	NU (Tunneling on one side)			0.008 @ 82°	Failed during proof
3W3-2	0.0164	0.1443	0.113	0.0176	121.0	33.2	30.0	0.95	0.86	NI	--	NV				Failed in grips during proof
3W3-4	0.0179	0.1329	0.129	0.0188	127.0	33.2	33.9	0.95	0.97	0.95	SG, CG	NU	0.002	0.001		
Heat Affected Zone																
3W3-7	0.0151	0.1663	0.091	0.0162	121.8	33.1	30.2	1.00	0.91	NI	--	NU			0.004 @ 78°	Failed during proof
3W3-5	0.0198	0.1905	0.104	0.0213	131.3	33.1	37.4	1.00	1.13	NI	--	NV				Failed during proof
3W3-8	0.0169	0.1616	0.105	0.0178	125.4	31.4	32.5	0.95	0.98	0.88	SG	NV				

*All hold times 15 seconds.

CODE:

NI - no indication; NU - nonuniform;
SG - strain gage; T - tunneling;
CG - compliance gage; NV - no visible growth indication.
U - uniform flaw growth;

Table A-16 Proof Test Data for 0.030-inch 6Al-4V Titanium Tested in Water

SPECIMEN NO.	FLAW SIZE				PROOF STRESS (psi)	STRESS INTENSITY, K_{Ii} (ksi$\sqrt{in.}$)		STRESS INTENSITY RATIO (K_{Ii}/K_{Ic})		FLAW GROWTH INITIATION		PROOF GROWTH				COMMENTS*
	DEPTH, a (in.)	LENGTH, 2c (in.)	SHAPE a/2c	a/Q		DESIRED	ACTUAL	DESIRED	ACTUAL	$\%K_{Ic}$	METHOD	TYPE	GROWTH (in.) AT INDICATED ANGLE 0° (Δa)	90° ($\Delta 2c$)	Ψ	
Parent Metal																
3CP-15	0.0214	0.1880	0.114	0.0225	141.1	39.6	41.3	1.00	1.04	NI	--	NU	0.002	0.001		
3CP-16	0.0177	0.1712	0.103	0.0190	138.2	37.6	37.2	0.95	0.94	0.92	--	NV				
Weld Centerline																
3W4-1	0.0166	0.1540	0.108	0.0189	129.5	34.9	34.5	1.00	0.99	0.93	SG	NU			0.001 @ 76°	Failed during proof
3W4-3	0.0163	0.1488	0.148	0.0164	126.6	33.2	31.6	0.95	0.91	NI	--	NU	0.001	0.003	0.002 @ 82°	
3W4-5	0.0178	0.1480	0.120	0.0191	125.1	33.2	33.7	0.95	0.97	0.93	SG	NV				
Heat Affected Zone																
3W5-3	0.0183	0.1498	0.122	0.0188	129.1	33.1	34.5	1.00	1.04	NI	--	NU	0.002	0.0004	0.012 @ 82°	
3W4-8	0.0188	0.1540	0.122	0.0202	126.4	31.4	35.0	0.95	1.06	0.92	SG	NV				

CODE:

NI - no indication; NU - nonuniform;
SG - strain gage; T - tunneling;
CG - compliance gage; NV - no visible growth indication.
U - uniform flaw growth;

*All hold times 15 seconds.

Table A-17 Proof Test Data for 0.030-inch 6A&-4V Titanium Tested in Liquid Nitrogen

SPECIMEN NO.	FLAW SIZE				PROOF STRESS (ksi)	STRESS INTENSITY, K_{Ii} (ksi$\sqrt{in.}$)		STRESS INTENSITY RATIO (K_{Ii}/K_{Ic})		FLAW GROWTH INITIATION		PROOF GROWTH				COMMENTS*
	DEPTH, a (in.)	LENGTH, 2c (in.)	SHAPE a/2c	a/Q		DESIRED	ACTUAL	DESIRED	ACTUAL	%K_{Ic}	METHOD	TYPE	GROWTH (in.) AT INDICATED ANGLE 0° (Δa)	90° (Δ2c)	Ψ	
Parent Metal																
3CP-21	0.0164	0.0557	0.294	0.0110	178.8	41.0	36.6	1.00	0.89	0.89	CG	T (on one side of flaw)			0.004 @ 75°	Starter flaw growth incomplete
3CP-20	0.0115	0.0478	0.241	0.0088	182.8	39.0	33.5	0.95	0.82	NI	--	NU	0.0006	0.001		
3CP-19	0.0105	0.0480	0.219	0.0085	188.8	34.8	33.9	0.85	0.83	NI	--	U	0.001	0.002		
Weld Centerline																
3W4-6	0.0138	0.0582	0.237	0.0106	186.0	40.7	37.4	1.00	0.92	NI	--	NU	0.0006	0.0008	0.002 @ 75°	
3W4-2	0.0123	0.0503	0.245	0.0092	182.0	38.7	34.1	0.95	0.84	NI	--	NV				
3W3-6	0.0115	0.0550	0.209	0.0096	213.1	34.6	40.7	0.85	1.00	NI	--	NU			0.0006 @ 60°	
Heat Affected Zone																
3W5-1	0.0116	0.0497	0.233	0.0090	186.2	36.6	34.5	1.00	0.94	NI	--	NV				
3W4-4	0.0116	0.0546	0.212	0.0094	180.4	34.8	34.1	0.95	0.93	NI	--	NV				
3W3-9	0.0100	0.0345	0.290	0.0069	202.2	31.1	32.7	0.85	0.89	NI	--	NV				Failed during proof

*All hold times 15 seconds.

CODE:

NI - no indication; NU - nonuniform;
SG - strain gage; T - tunneling;
CG - compliance gage; NV - no visible growth indication.
U - uniform flaw growth;

Table A-18 Cyclic Crack-Extension Properties for 0.090-inch 6Al-4V Titanium

SPECIMEN NO.	FLAW SIZE INITIAL DEPTH, a (in.)	INITIAL LENGTH, 2c (in.)	INITIAL a/Q	FINAL DEPTH, a (in.)	FINAL LENGTH, 2c (in.)	FINAL a/Q	STRESS INTENSITY ($ksi\sqrt{in.}$) INITIAL	FINAL	AVERAGE	CYCLES, N	CRACK EXTENSION, da/Q_{avg} (μin.)	CRACK-EXTENSION RATE $d(a/Q_{avg})/dN$ (μin./cycle)	COMMENTS
PARENT METAL													
9CP-7	0.0696	0.2355	0.0458	0.0730	0.2428	0.0474	43.8	44.6	44.2	100	2222	22.2	
9CP-12	0.0604	0.2909	0.0405	0.0668	0.2215	0.0439	41.2	43.0	42.1	300	4267	14.2	
9CP-21	0.0492	0.1316	0.0272	0.0595	0.1595	0.0329	33.8	37.1	35.4	500	5690	11.4	
9CP-30	0.0453	0.2420	0.0378	0.0566	0.2567	0.0442	39.8	43.0	41.4	500	11,854	23.7	
9CP-31	0.0467	0.2389	0.0396	0.0663	0.2682	0.0491	40.7	45.5	43.1	500	15,430	30.9	
9CP-8	0.0580	0.1461	0.0305	0.0689	0.1815	0.0374	35.8	39.5	37.7	500	5828	11.7	
9CP-20	0.0607	0.1555	0.0323	0.0646	0.1647	0.0344	36.9	37.9	37.4	130	2074	16.0	
9CP-15	0.0494	0.1171	0.0245	0.0567	0.1421	0.0295	32.1	35.2	33.6	500	3706	7.4	
9CP-26	0.0493	0.2440	0.0401	0.0597	0.2558	0.0452	41.0	43.5	42.3	400	8125	20.3	
9CP-27	0.0380	0.2298	0.0333	0.0489	0.2486	0.0400	37.3	41.0	39.2	500	9237	18.5	
9CP-45	0.0316	0.0948	0.0190	0.0388	0.1050	0.0216	28.3	30.1	29.2	500	4200	8.4	
9CP-47	0.0268	0.0844	0.0168	0.0322	0.0884	0.0181	26.6	27.6	27.1	500	3200	6.4	
9DP-9	0.0332	0.0945	0.0193	0.0387	0.1032	0.0213	28.5	29.9	29.2	500	3107	6.2	
WELD CENTERLINE													
9W11-2	0.0324	0.0902	0.0189	0.0464	0.1015	0.0218	28.1	30.3	29.2	500	7250	14.6	
9W10-6	0.0345	0.1096	0.0224	0.0385	0.1204	0.0247	30.7	32.1	31.4	200	2580	13.0	
9W15-2	0.0255	0.0872	0.0173	0.0316	0.0920	0.0192	27.0	28.3	27.6	500	3910	7.8	
9W10-4	0.0335	0.0931	0.0196	0.0367	0.1171	0.0290	28.6	34.8	31.7	500	2170	4.3	
9W5-1	0.0707	0.1893	0.0402	0.0770	0.2221	0.0464	41.0	44.0	42.5	101	3684	36.5	
9W2-1	0.0612	0.1702	0.0357	0.0750	0.2161	0.0449	38.7	43.4	41.0	300	8165	27.2	
9W7-1	0.0507	0.2733	0.0445	0.0570	0.2793	0.0475	41.3	44.6	41.4	100	5384	53.8	
9W7-2	0.0465	0.2607	0.0411	0.0545	0.2900	0.0470	41.6	44.4	43.0	100	6986	69.8	
9W10-3	0.0433	0.2508	0.0387	0.0834	0.3105	0.0600	40.3	50.1	45.2	500	31,825	63.6	
9W2-3	0.0540	0.1950	0.0380	0.0637	0.2085	0.0422	39.9	42.1	41.0	200	6643	33.2	
9W2-4	0.0670	0.1865	0.0387	0.0778	0.2141	0.0455	40.3	43.6	41.9	222	6242	28.1	
9W3-3	0.0630	0.1772	0.0373	0.0824	0.2030	0.0434	39.5	42.6	42.1	300	11,055	36.8	
9W8-3	0.0462	0.2535	0.0405	0.0740	0.2780	0.0536	41.2	47.4	44.3	391	22,063	56.4	
9W8-4	0.0439	0.2334	0.0378	0.0662	0.2737	0.0509	39.7	46.3	43.0	300	18,130	60.4	
HEAT AFFECTED ZONE													
9W11-5	0.0395	0.1298	0.0260	0.0453	0.1434	0.0290	33.0	34.8	33.9	300	3766	12.7	
9W11-3	0.0370	0.1158	0.0234	0.0420	0.1249	0.0256	31.3	32.8	32.0	300	3105	10.3	
9W11-1	0.0320	0.1130	0.0221	0.0390	0.1184	0.0242	30.5	31.9	31.2	214	4575	21.5	
9W10-5	0.0223	0.0850	0.0162	0.0248	0.0920	0.0176	26.0	27.2	26.6	500	1785	3.6	
9W15-6	0.0228	0.0904	0.0169	0.0267	0.0948	0.0184	26.6	27.8	27.2	200	2785	14.0	
9W15-3	0.0310	0.1028	0.0204	0.0488	0.1413	0.0290	29.3	34.8	32.1	500	11,120	22.3	
9W12-6	0.0687	0.1730	0.0363	0.0763	0.1987	0.0412	39.1	41.6	40.3	100	4064	40.6	
9W4-1	0.0508	0.1352	0.0283	0.0624	0.1762	0.0365	34.4	41.6	38.0	500	6628	13.2	
9W3-5	0.0524	0.1244	0.0265	0.0622	0.1531	0.0325	33.4	36.8	35.1	500	5051	10.1	
9W7-5	0.0494	0.2723	0.0430	0.0880	0.5438	0.0467	42.5	44.2	43.4	100	4632	46.3	
9W10-2	0.0417	0.2381	0.0365	0.0621	0.2728	0.0481	39.1	42.8	40.9	400	16,790	42.4	
9W6-5	0.0641	0.1716	0.0358				38.7			460			Cracked Through During Cycling
9W5-4	0.0560	0.1431	0.0304	0.0678	0.1777	0.0374	35.6	39.5	37.6	420	6259	14.9	
9W9-1	0.0435	0.2476	0.0381	0.0845	0.4114	0.0693	40.0	53.8	46.9	270	34,745	12.9	
9W9-2	0.0480	0.2539	0.0407	0.0681	0.2885	0.0520	41.4	46.7	44.1	300	16,064	55.9	

Note: Stress ratio (R) = 0.01; σ_{max} = 105ksi.

Table A-19 Cyclic Crack-Extension Properties for 0.060-inch 6Al-4V Titanium

SPECIMEN NO.	FLAW SIZE						STRESS INTENSITY ($ksi\sqrt{in.}$)			CYCLES, N	CRACK EXTENSION da/Q_{avg} (μin.)	CRACK EXTENSION RATE, $d(a/Q_{avg})/dN$ (μin./cycle)	COMMENTS
	INITIAL			FINAL									
	DEPTH, a (in.)	LENGTH, 2c (in.)	a/Q	DEPTH, a (in.)	LENGTH, 2c (in.)	a/Q	INITIAL	FINAL	AVERAGE				
Parent Metal													
6CP-3	0.0405	0.1302	0.0230	0.0480	0.1366	0.0279	31.1	34.2	32.7	100	4310	43.1	
6CP-4	0.0447	0.1127	0.0235	0.0514	0.1307	0.0271	31.3	33.8	32.5	500	3526	7.1	
6CP-6	0.0364	0.2244	0.0319	0.0528	0.2634	0.0429	36.7	42.4	39.6	400	13,780	34.5	
6CP-11	0.0294	0.2137	0.0270	0.0354	0.2316	0.0319	33.6	36.6	35.1	100	5455	54.5	
6DP-18	0.0508	0.1524	0.0306	0.0578	0.1874	0.0368	35.8	39.3	37.6	500	4347	8.7	
6CP-26	0.0499	0.1345	0.0282	0.0565	0.1732	0.0342	34.4	37.9	36.2	440	3859	8.7	
6DP-3	0.0420	0.2322	0.0356	0.0487	0.2452	0.0396	38.7	40.8	39.8	200	5537	27.7	
6CP-27	0.0295	0.2089	0.0270	0.0410	0.2182	0.0339	33.6	37.7	35.7	500	10,000	20.0	
6DP-11	0.0290	0.0862	0.0174	0.0318	0.0970	0.0194	27.0	28.5	27.7	73	1686	23.3	
6DP-12	0.0218	0.0908	0.0161	0.0285	0.0986	0.0190	26.0	28.3	27.1	500	4718	9.4	
6DP-6	0.0326	0.0928	0.0190	0.0362	0.1032	0.0210	28.3	29.7	29.0	500	2093	4.2	
6DP-9	0.0243	0.0969	0.0176	0.0250	0.0977	0.0256	27.2	27.4	27.3	500	504	1.0	
6CP-9	0.0522	0.1557	0.0314	0.0597	0.1939	0.0380	36.2	39.9	38.1	500	4032	8.1	
6CP-17	0.0482	0.1344	0.0274	0.0529	0.1588	0.0321	33.8	36.6	35.2	250	2756	11.0	
6DP-13	0.0447	0.2212	0.0363	0.0552	0.2449	0.0425	39.1	42.2	40.7	300	8300	27.6	
6CP-22	0.0376	0.2071	0.0319	0.0551	0.2429	0.0421	36.6	42.0	39.3	475	14,056	29.5	
6CP-28	0.0487	0.1365	0.0277	0.0533	0.1717	0.0339	34.0	37.7	35.8	503	2762	5.4	
6DP-5	0.0408	0.2242	0.0346	0.0554	0.2483	0.0426	38.1	42.2	40.1	441	11,770	26.6	
6CP-29	0.0298	0.2090	0.0273	0.0354	0.2183	0.0313	33.8	36.2	35.0	500	5045	10.0	
Weld Centerline													
6W3-8	0.0525	0.1392	0.0293	0.0540	0.1535	0.0323	35.0	36.8	35.9	100	867	8.7	
6W5-4	0.0340	0.2159	0.0315				36.2			104			Cracked through during cycling
6W5-2	0.0401	0.2196	0.0352				38.5			65			Cracked through during cycling
6W3-9	0.0613	0.1639	0.0344				37.9			220			Cracked through during cycling
6W7-2	0.0241	0.0919	0.0177	0.0241	0.0919	0.0177	27.2	27.2	27.2	500	0	0	No flaw growth
6W6-4	0.0293	0.0850	0.0178	0.0305	0.0897	0.0186	27.2	27.8	27.5	300	727	2.4	
6W9-9	0.0282	0.0825	0.0172	0.0294	0.0840	0.0175	26.8	27.0	26.9	175	723	4.1	
Heat Affected Zone													
6W3-4	0.0540	0.1319	0.0277	0.0556	0.1354	0.02585	34.0	34.6	34.3	100	820	8.2	
6W5-8	0.0323	0.2147	0.0294	0.0478	0.2349	0.0389	35.0	40.3	37.7	500	13,300	26.6	
6W5-5	0.0352	0.2036	0.0306	0.0424	0.2127	0.0350	35.8	38.3	37.0	157	6101	38.9	
6W3-5	0.0485	0.1372	0.0282	0.0561	0.1683	0.0344	34.4	37.9	36.2	380	4537	11.9	
6W5-9	0.0376	0.2182	0.0324	0.0435	0.2281	0.0365	36.8	39.1	38.0	167	5021	30.0	
6W9-6	0.0293	0.0916	0.0183	0.0338	0.1010	0.0205	27.6	29.3	28.4	260	2760	10.6	
6W6-7	0.0263	0.0868	0.0171	0.0303	0.0955	0.0192	26.8	28.5	27.6	160	2564	16.0	
6W8-6	0.0255	0.0890	0.0172	0.0265	0.0927	0.0179	26.8	27.4	27.1	500	632	1.3	
6W7-3	0.0176	0.0815	0.0140	0.0207	0.0844	0.0153	24.2	25.4	24.8	500	2366	4.7	
6W7-1	0.0201	0.0768	0.0144	0.0244	0.0812	0.0161	24.6	26.0	25.3	500	2945	5.9	

Note: Stress ratio (R) = 0.01; σ_{max} = 105 ksi.

Table A-20 Cyclic Crack-Extension Properties for 0.030-inch 6Al-4V Titanium

SPECIMEN NO.	FLAW SIZE						STRESS INTENSITY ($ksi\sqrt{in.}$)			CYCLES, N	CRACK EXTENSION da/Q_{avg} (μin.)	CRACK EXTENSION RATE, $d(a/Q_{avg})/dN$ (μin./cycle)	COMMENTS
	INITIAL			FINAL									
	DEPTH, a (in.)	LENGTH, 2c (in.)	a/Q	DEPTH, a (in.)	LENGTH, 2c (in.)	a/Q	INITIAL	FINAL	AVERAGE				
Parent Metal													
3CP-13	0.0172	0.0994	0.0154	0.0181	0.1734	0.0185	25.4	27.8	26.6	100	1415	14.2	
3CP-15	0.0229	0.1893	0.0222	0.0268	0.1945	0.0250	30.5	32.4	31.5	141	3714	26.3	
3CP-16	0.0177	0.1712	0.0176	0.0279	0.1950	0.0256	27.2	32.8	30.0	327	9807	29.9	
3CP-21	0.0164	0.0591	0.0114	0.0178	0.0753	0.0135	21.9	23.8	22.9	500	1021	2.0	
3CP-20	0.0127	0.0507	0.0093	0.0127	0.0507	0.0093	19.7	19.7	19.7	500	0	0	No cyclic growth
Weld Centerline													
3W3-4	0.0179	0.1392	0.0169				26.6			100			Cracked through during cycling
3W4-3	0.0220	0.1686	0.0210				29.7			42			Cracked through during cycling
3W4-6	0.0138	0.0600	0.0109	0.0167	0.0802	0.0138	21.3	23.9	22.6	200	2339	11.7	
3W4-2	0.1230	0.0503	0.0094	0.0133	0.0538	0.0101	19.8	20.5	20.2	500	763	1.5	
3W3-6	0.1120	0.0526								500	0	0	
Heat Affected Zone													
3W3-8	0.0169	0.1616	0.0167				26.4			100			Cracked through during cycling
3W5-3	0.0254	0.1680	0.0231				31.1			168			Cracked through during cycling
3W4-8	0.0188	0.1546	0.0181	0.0263	0.1602	0.0233	27.6	31.3	29.4	115	7436	64.6	
3W5-1	0.0116	0.0497	0.0092	0.0130	0.0539	0.0098	19.6	20.2	19.9	475	1077	2.2	
3W4-4	0.0126	0.0546	0.0098	0.0142	0.0567	0.0105	20.3	20.9	20.6	214	1212	5.7	

Note: Stress ratio (R) = 0.01

σ_{max} = 105 ksi